# Understanding PPA-completeness

Xiaotie Deng [a,*], Jack R. Edmonds, Zhe Feng [b], Zhengyang Liu [c], Qi Qi [d], Zeying Xu [e]

[a] *Center on Frontiers of Computing Studies, Peking University, Beijing, PR China*
[b] *John A. Paulson School of Engineering and Applied Sciences, Harvard University, Cambridge, MA, USA*
[c] *Department of Computer Science, Shanghai Jiao Tong University, Shanghai, PR China*
[d] *Department of Industrial Engineering and Decision Analytics, Hong Kong University of Science and Technology, Hong Kong*
[e] *Department of Mathematics, Shanghai Jiao Tong University, Shanghai, PR China*

## ARTICLE INFO

## ABSTRACT

We show that computation of the SPERNER problem is PPA-complete on the Möbius band under proper boundary conditions, settling a long term open problem. Further, the same computational complexity results extend to other discrete fixed points on the Möbius band, such as the Brouwer fixed point problem, the DPZP fixed point problem and a simple version of the Tucker problem, as well as the projective plane and the Klein bottle. We expect it opens up a new route for further studies on the related combinatorial structures.

© 2020 Elsevier Inc. All rights reserved.

## 1. Introduction

The Nash equilibrium is a stable state in non-cooperative games, at which no player has incentive to change its strategy even if it knows the equilibrium strategies of others. As a computational method, the celebrated Lemke-Howson algorithm [1] finds a graph structure in the shape of a path to derive a solution for any two-player game. It starts from a degree one node *s* and continues to move along the unused edge along the path. Eventually, another node of degree one must be reached, which corresponds to a Nash equilibrium.

Such an implicit path graph has also demonstrated its usefulness in many other interesting problems. It has also become widely known as the path-following paradigm, one of the most successful algorithmic paradigms in mathematical programming and operations research. Cottle and Dantzig [2], for example, have studied and used the approach extensively to solve linear complementary problems.

A closer examination at the graph structure for any bimatrix game reveals a directed graph (digraph) with neither in-degree nor out-degree no more than one. Every node of total degree one, including those with out-degree one and in-degree zero, corresponds to a Nash equilibrium (even though Lemke-Howson always finds one with in-degree one and out-degree zero).

To capture the time complexity of such problems with an implicit directed graph of paths and cycles, potentially of an exponential size, Papadimitriou [3] introduced the class PPAD (Polynomial Parity Argument, the Directed version), which

---

* Corresponding author.
  *E-mail addresses:* xiaotie@pku.edu.cn (X. Deng), jack.n2m2m6@gmail.com (J.R. Edmonds), zhe_feng@g.harvard.edu (Z. Feng), zhengyang@bit.edu.cn (Z. Liu), kaylaqi@ust.hk (Q. Qi), zane_xu@sjtu.edu.cn (Z. Xu).

now includes finding a Nash equilibrium for two-player games as a complete problem (see, e.g., Chen et al. [4]) as well as many other related problems. Kintali [5] provides a list of 25 of the most well-known PPAD-complete problems.

In sharp contrast, a sister (and more inclusive) complexity class PPA (Polynomial Parity Argument) for the undirected graph, which was defined in the same seminal paper of Papadimitriou [3] has not received as much attention, despite of many interesting known PPA problems. Indeed, there are many interesting existence theorems in graph theory, combinatorics and number theory for which the computational problems belong to the PPA class. Examples include Smith's theorem by Thomason [6] and related existentially polytime (graph) theorems by Cameron and Edmonds [7], Chevalley's theorem by Chevalley [8] and Alon's Combinatorial Nullstellensatz by Alon [9], among others. Remarkably, the problem of factoring an integer has recently been proved by Jerábek [10] to belong to the PPA class (via randomized reductions). The inclusion of this fundamental and critical problem gives the class a new meaning.

Unfortunately, we know of few PPA-complete problems besides the generic one and certain versions of Sperner's problem for rather esoteric non-orientable bodies. Some ten years after the introduction of the PPA class, Grigni [11] proposed the important idea that the right geometric context for PPA consists of non-orientable bodies and showed that a version of Sperner's problem in the non-orientable three-dimensional (3D) space is PPA-complete. A few years later, Friedl et al. [12] strengthened this work of Grigni to a non-orientable and locally two-dimensional (2D) orientable space.

In general, it would be desirable to have a larger collection of PPA-complete problems (such as what we have for PPAD) and eventually include integer factorization problem in the collection. The progress has been slow: another ten years have passed since the work of Friedl et al. [12] without any progress in our understanding of the PPA-complete class which many scientists are interested in.

*Main results and contributions*

In this paper, we prove that finding a Sperner triangle in a triangulation of the Möbius band satisfying an appropriate boundary condition is PPA-complete. This result has allowed several related PPA-complete problems to be identified for an array of different types of discrete fixed points, such as DPZP, Sperner, Brouwer and simple Tucker problems. The main results are the proofs of the PPA-completeness of the following problems.

- Discrete fixed points on a 2D Möbius band.
- Discrete fixed points in other non-orientable spaces.
- Discrete fixed points in high-dimensional non-orientable spaces.

Furthermore, we prove the matching oracle complexity of discrete fixed points in non-orientable spaces.

Together, these results establish the Möbius band, and non-orientable spaces in general, are the right space to consider the PPA-complete class, inheriting the one dimension nature of the undirected graphs of cycles and paths. Therefore, we call the undirected version of such graph problem AEUL (another endpoint of undirected lines), corresponding to PPA, and its directed graph version AEDL (another endpoint of directed lines), corresponding to PPAD.

The simple structure of Möbius band improves our current understanding of the PPA-complete class and concludes the question put forth by Grigni to find a simple and natural Sperner's lemma which is PPA-complete in a non-orientable space.

For ease of presentation, we start by embedding a PPA graph in the 2D Möbius band in a way that yields a special type of discrete fixed point for the PPA-hardness proof while it is easy to be shown in PPA. This type of discrete fixed point is originally defined in Chen and Deng [13] and called DPZP (Direction Preserving Zero Points) by Deng et al. [14]. A color function in DPZP returns for each grid point a color value in $\{0, \pm 1, \pm 2\}$ and forbids grid points within a unit distance in the infinity metric to have the same absolute value of opposite signs. The goal of DPZP is to find a zero point in the exponential size grid $2^n \times 2^n$, with appropriate boundary condition for the grid to satisfy the Möbius property and a parity property. Our PPA-complete proof for DPZP on the Möbius band further derives as corollaries the PPA-completeness results of other versions of fixed points on the Möbius band, such as Sperner's problem, Brouwer's problem and the simple version of Tucker.

The PPA-complete proof for DPZP in the 2D Möbius band is developed upon several important ideas such as the mod 2 index in Chen and Deng [13], the planar layout method of exponential size paths and cycles in polynomial time, as well as the edge intersection breaking technique in Chen and Deng [15]. Further, it exploits the Möbius band's face reversing property to allow certain changes in direction on the linking edges. An extension of the *topological index* plays an important role in the membership proof of the fixed points on the Möbius band. In particular, along with several important technical details, a dicephalic snake lemma is crucial for the padding and folding to create a higher dimensional fixed point on a non-orientable grid in order to reduce the problem to one of constant side lengths.

Several difficulties stopped the results to be discovered in the past. First, the embedding of the directed paths and cycles on a 2D plane places the edges on the AEDL instance in an orderly manner, so that we can color vertices properly. Such a natural direction does not exist for the undirected graph. Here we define a local order of the edges in a consistent way to place the undirected edges on the 2D plane so that we can color the vertices properly to guarantee a solution to AEUL matches with a fully colored base triangle. Second, as we order the edges of the graph direct as in the above, we need to connect them properly (head to tail) to form directed paths and directed cycles in the constructed digraph. As the graph is potentially exponential in size, the proper orientation of each edge needs to be locally computable in polynomial time.

**Table 1**
Summary I: complexity.

|          | Orientable 2D space      | Non-orientable 2D space                     |
|----------|--------------------------|---------------------------------------------|
| Sperner  | PPAD-complete ([15])     | PPA-complete (this paper)                   |
| Brouwer  | PPAD-complete ([15])     | PPA-complete (this paper)                   |
| DPZP     | PPAD-complete ([14])     | PPA-complete (this paper)                   |
| Tucker   | PPA-complete ([21])      | PPA-complete (simple Tucker in this paper)  |

**Table 2**
Summary II: Oracle model complexity.

|          | Orientable 2D space         | Non-orientable 2D space           |
|----------|-----------------------------|-----------------------------------|
| Sperner  | $\Theta(N^{d-1})$           | $\Theta(N^{d-1})$ (this paper)    |
|          | 2D Lower: [22]              |                                   |
|          | 2D Upper: [12]              |                                   |
|          | Other dimensions: [14]      |                                   |
| Brouwer  | $\Theta(N^{d-1})$ ([14])    | $\Theta(N^{d-1})$ (this paper)    |
| DPZP     | $\Theta(N^{d-1})$ ([13])    | $\Theta(N^{d-1})$ (this paper)    |
| Tucker   | $\Theta(N^{d-1})$ ([14])    | $\Theta(N^{d-1})$ (this paper)    |

Third, eventually we need to remove the directions so that the orientation of the embedding of undirected lines and cycles through the oriented local space will be removed.

To handle those difficulties, a key idea is to use the face reversing property of the Möbius band, which is introduced at the boundary of the grid with the use of a direction reversing line to stitch the lines and cycles back together. The colorings of the triangulated Möbius band are then done locally with the help of the local orientations of corresponding lines and cycles, which are un-oriented globally through the direction reversing line placed on the two opposite boundary.

The main line of ideas can be stated here but very complicated to make through verbally in sufficient details. We will make the precise presentation in the subsequent sections in mathematical terms.

*Related literatures*

The standard Sperner's problem, the 3D-Sperner, is among the first natural problems proved to be PPAD-complete by Papadimitriou [3]. The problem was extended to the 2D-Sperner in Chen and Deng [15]. Grigni [11] proposed the brilliant idea of using a non-orientable space to model the 3D-Sperner as a PPA-complete problem. To our best knowledge, the only other known PPA-complete problem before this work was the Sperner problem on a sophisticated locally 2D structure in Friedl et al. [12].

The algorithm of Lemke and Howson [1] for Nash equilibrium computation has started a path-following paradigm. However, Savani and von Stengel [16] found a worst case exponential lower bound for this algorithm. Hirsch et al. [17] showed that finding a Brouwer's fixed point requires exponential time under the oracle model. Chen and Deng [13] further showed that the problem had a tight exponential time bound. Deng et al. [14] extended the tight exponential time bound result to include several discrete versions of the fixed point problem.

For the PPA class, Krawczyk [18] and Cameron [19] showed that the SMITH problem takes exponential time to solve using the path-following method. The result has been extended to related problems, such as an exponential time bound for finding the second perfect matching on Eulerian graphs by Edmonds and Sanità [20]. An extensive discussion on related problems can be found in Cameron and Edmonds [7].

Subsequent to the appearance of a preliminary version of this work, Aisenberg et al. [21] applied similar ideas to prove that the general version of the 2D-Tucker in the Euclidean space is PPA-complete, which was the first PPA-complete discrete fixed point problem in the Euclidean space. Those two types of results separate, in the context of computational complexity, various discrete types of fixed points. In particular, 2D Tucker on Euclidean space is the same, in terms of computational complexity for finding a solution, as other discrete fixed points on the non-orientable space.

Table 1 and Table 2 compare the previous results and those of this work.

*Organization of presentation*

The paper proceeds as follows: In Section 2, we will introduce the necessary definitions and notations. In Section 3, we prove a key result, the PPA-completeness of the Möbius DPZP problem and demonstrate its applications. In Section 4, we apply our main result to other non-orientable spaces, including the projective plane and the Klein bottle. We prove the PPA-completeness of the problem of finding another fixed point in the projective plane and on the Klein bottle. In Section 5, we extend our work to prove a high-dimensional non-orientable version of fixed points. In Section 6, we obtain tight bounds for the oracle model of the computational problem for discrete fixed points in non-orientable spaces. In Section 7, we discuss the generality of the results obtained here in related settings. Finally, we comment on the potentials of techniques developed here for expanding our future understandings the computational complexity class of PPA.

## 2. Preliminaries and definitions

PPA (Polynomial Parity Argument class) is a class of search problems based on an exponential size graph consisting of nodes of maximum degree two, with a given node of degree one. The problem asks for an output of another node of degree one, which is guaranteed to exist by the parity argument. More formally, we define it by a complete problem, named AEUL (another end of undirected lines) as follows:

**Definition 1.** $AEUL(T_n, C_n, 0^n)$: Let the input circuit $T_n$ of polynomial size in $n$ take $u \in C_n = \{0, 1\}^n$ and returns an output $T_n(u)$ in one of the forms $\langle v, w \rangle, \langle v \rangle$, or $\langle \rangle$ where $v \to w$ being a directed edge from $v$ to $w$, and $v, w \in C_n \setminus \{u\}$. $0^n$ is a given configuration of degree one: $|T_n(0^n)| = 1$. The search problem is to find another configuration $v$ of degree one, $v \neq 0^n$ and $|T_n(v)| = 1$.

Comment: We say $AEUL(T_n, C_n, 0^n)$ is represented by $T_n$ in polynomial time in $n$. We do so subsequently in similar cases where the structure is exponential but we have a polynomial time algorithm to access a node and its adjacent data.

We comment that AEUL can be viewed as a promise problem [23]. According to [24], the promise here restricts that there is no inconsistency for the outputs of the input circuit $T_n$. That is, if v is in $T_n(u)$ then u is also in $T_n(v)$. Otherwise, the problem AEUL without such a promise would in its solution need to output an such inconsistency or a desired node of degree one. We comment that all the problems studied here are of the promise version.

*Möbius band*

The Möbius band is obtained by merging the left and right sides of a rectangle after twisting it 180 degrees clockwise or counterclockwise to form a band with one boundary and one surface. Therefore, it is non-orientable. More formally,

**Definition 2** (*Möbius band* $B_{N,M}$). Let $V_{N,M} = \{\mathbf{p} = (p_1, p_2) \in \mathbb{Z}^2 : -N \leq p_1 \leq N, -M \leq p_2 \leq M\}$. A Möbius band is obtained by twisting $V_{N,M}$ 180 degrees clockwise and then joining every vertex $(N, y)$ with $(-N, -y)$ to form a loop. A function $f$ is defined on the *Möbius band* $B_{N,M}$ iff $\forall y : -M \leq y \leq M$. We have $f((N, y)) = f((-N, -y))$ on $V_{N,M}$.

**Definition 3** (*Triangulation*). For each $i, j \in \mathbb{Z} : -N \leq i < N, -M \leq j < M$, we link $(i, j)$ with $(i + 1, j + 1)$ on the grids $V_{N,M}$ (and $B_{N,M}$).

We call every unit square in the standard triangulated grid $V_{N,M}$ a *base square*, every triangle of unit side length a *base triangle*, and every one of its edge a *base edge*.

*Index*

We now redefine the *index*, originally defined by [25] and [26], and adopt it for the non-orientable space $B_{N,M}$. The definition and discussion here will be general enough to be used for the following coloring functions, unless specifically stated.

**Definition 4** (*Index of an edge and a triangle*). Consider a triangulated Möbius grid $B_{N,M}$, and a coloring $\phi : B_{N,M} \to R$ on all vertices in $B_{N,M}$ with $1, 2 \in R$, where $R$ is the set of colors. Let the *index* of an edge $index(e(u, v), \phi)$ be 1 if the $\{\phi(u), \phi(v)\} = \{1, 2\}$, and 0 otherwise. The *index* of a base triangle $index(\delta = \{e_1, e_2, e_3\}, \phi)$ is the sum of the indices of its three edges $\sum_{i=1}^{3} index(e_i, \phi)$ (mod 2).

We are now ready to define the index on a Möbius band.

**Definition 5** (*Index of the triangulated* $B_{N,M}$). Given a triangulated Möbius grid $B_{N,M}$, a coloring $\phi : B_{N,M} \to R$ with $R \ni 1, 2$. The *index* of $B_{N,M}$ is defined as

$$\text{index}(B_{N,M}, \phi) := \sum_{\delta \text{ is a base triangle } \in B_{N,M}} \text{index}(\delta, \phi) \pmod{2}$$

Immediately, we can derive the following lemma concerning indices on the Möbius band.

**Lemma 1.**

$$\text{index}(B_{N,M}, \phi) = \sum_{e \in \partial B_{N,M}} \text{index}(e, \phi) \pmod{2},$$

where $\partial B_{N,M}$ is the boundary of $B_{N,M}$, that is, $\partial B_{N,M} := \{(p_1, \pm M) \in \mathbb{Z}^2 : -N \leq p_1 \leq N\}$.

**Proof.** As any internal base edge appears in the calculation of indices of two base triangles, the summation of their indices is either 0 or 2, which equals to 0 (mod 2). The proof is complete. □

*DPZP*

Before we define a Möbius version of the original direction-preserving zero point, we introduce several properties of the functions used here first.

**Definition 6** *(Möbius feasible function).* We say that a function $f(\cdot)$ defined on $B_{N,M}$ is *feasible* if it satisfies the Möbius condition $f((N, y)) = f((-N, -y)), \forall y \in \mathbb{Z}, -M \le y \le M$.

**Definition 7** *(Möbius (numerical) direction-preserving function).* A function $f : B_{N,M} \to \{0, \pm1, \pm2\}$ is *(numerical) direction-preserving* if for any $\mathbf{p}, \mathbf{q} \in B_{N,M}$ where $||\mathbf{p} - \mathbf{q}||_\infty = 1$ and $f(\mathbf{p}) \ne 0$, we have $f(\mathbf{p}) + f(\mathbf{q}) \ne 0$.

Comment: Here $\pm i$ may be viewed as numerical counter parts of $\pm e_i$, the coordinate vectors with the $i$-th value $\pm1$ and 0 otherwise. In this form, a function is direction-preserving if no two neighbors (with $\ell_\infty$ one) can be assigned opposite direction.

**Definition 8** *(Zero point base triangle).* A base triangle $\delta$ of a triangulated Möbius grid, given a function $f : B_{N,M} \to \{0, \pm1, \pm2\}$, is called a *zero point base triangle* of $f$ if $\{f(\mathbf{p}) : \mathbf{p} \in \delta\} = \{0, 1, 2\}$.

**Definition 9** *(Admissible boundary condition).* A function $F : B_{N,M} \to \{0, \pm1, \pm2\}$ is *admissible* if it satisfies the following boundary conditions:

- $F((0, M)) = -2;\ F((0, -M)) = 2$
- $F((i, M)) = F((-i, -M)) = -1$, for every $i \in \mathbb{Z}: 0 < i \le N$
- $F((-i, M)) = F((i, -M)) = 1$, for every $i \in \mathbb{Z}: 0 < i \le N$

**Definition 10** *(Möbius DPZP $(B_{N,M}, f; F)$).* Given a triangulated Möbius grid $B_{N,M}$ and a polynomial-time machine $F$ that represents a numeric direction-preserving feasible admissible function $f$ on $B_{N,M} : f(\mathbf{p}) \in \{0, \pm1, \pm2\}, \forall \mathbf{p} \in B_{N,M}$, the needed output is a vertex $\mathbf{p} : f(\mathbf{p}) = 0$.

We have the following lemma on the Möbius grid.

**Lemma 2.** *We have* index$(\delta, f) = 1$ *if and only if* $f(\delta) = \{0, 1, 2\}$. *Furthermore,* index$(B_{N,M}, f) = \sum_{e \in \partial B_{N,M}}$ index$(e, f)$ (mod 2), *where* $\partial B_{N,M}$ *is the boundary of* $B_{N,M}$.

**Proof.** First, a base triangle is of index 1 if and only if its vertices are colored $\{x, 1, 2\}$ where $x \notin \{1, 2\}$. As all vertices in a base triangle are of distance 1 in $\infty$-metric, $x$ cannot be $-1$ or $-2$ by the direction-preserving property. The only index 1 base triangle is $\{0, 1, 2\}$. □

Using the index on non-orientable surfaces, Lemma 3 immediately follows.

**Lemma 3.** *Möbius DPZP$(B_{N,M}, f; F)$ with an admissible boundary always has a zero point. Finding a zero point is a PPA problem.*

**Proof.** The structure of the proof goes as follows: We are proving that any DPZP instance can be solved by an solution to the AEUL instance constructed here. To construct an instance of AEUL, we define a node of AEUL as an edge of color (1,2) in the DPZP instance. Two vertices in the AEUL instance sharing an edge are two edges in the DPZP instance of color (1,2) (unordered) sharing a base triangle. The given degree one node of the AEUL instance is the unique edge on the boundary of the DPZP instance. Another end of lines in such an AUEL instance will be an edge $(1, 2)$ in a base triangle of three colors $(1, 2, x)$ where $x \notin \{1, 2\}$ in the DPZP instance. Also, $x$ cannot be $-1$ nor $-2$ by the direction preserving condition. We must have $x = 0$ which is the solution we sought for in the DPZP instance.

More formally, since we have only one edge with $(2, 1)$ on the boundary of the Möbius band for any DPZP function with an admissible boundary, the index of edges along the boundary is 1. Therefore, by Lemma 2, there is an odd number of zero point base triangles on the Möbius grid. Therefore, there is always a zero point on the Möbius grid.

To construct the instance of AEUL from the Möbius DPZP instance, we take the boundary edge $(2, 1)$ in Möbius DPZP instance as the origin node of the AEUL instance. Two edges of $\{1, 2\}$ colors in the same base triangle of the Möbius DPZP instance are connected in the AEUL instance. Any such edge in the Möbius DPZP instance is a leaf node of the AEUL instance if the edge is the single $\{1, 2\}$ edge in a base triangle of the Möbius DPZP instance.

Therefore, any base triangle of colors $\{0, 1, 2\}$ in the Möbius DPZP instance is an end node in some line of the AEUL instance, different from the given degree one node in the AEUL instance. Therefore, finding another end of lines in the AEUL instance constructed above leads to a zero point in the input instance of the DPZP problem. Therefore, DPZP belongs to the PPA class.   □

Next we present the results for other related discrete fixed point concepts on the Möbius band.

*Sperner*

We call the problem of finding a fully colored base triangle on the Möbius band $B_{N,M}$ the Möbius Sperner problem.

**Definition 11** *(Möbius Sperner($B_{N,M}, g; G$))*. Consider a triangulated Möbius grid $B_{N,M}$ and a polynomial-time machine $G$, which generates a feasible function $g$ from $B_{N,M}$ to $\{0, 1, 2\}$: $g(\mathbf{p}) = G(\mathbf{p}) \in \{0, 1, 2\}, \forall \mathbf{p} \in B_{N,M}$.
   Furthermore, we say that $G$ is admissible if it satisfies the following Möbius Sperner boundary condition.

- $G((0, M)) = 0$; $G((0, -M)) = 2$
- $G((i, M)) = G((-i, -M)) = 0$, for every $i \in \mathbb{Z}$: $0 < i \leq N$
- $G((-i, M)) = G((i, -M)) = 1$, for every $i \in \mathbb{Z}$: $0 < i \leq N$

The required output is a base triangle containing all three colors, which will be named ***Sperner base triangles***. In general, a fully colored base simplex is called a ***Sperner base simplex***.

**Lemma 4.** *On any admissible triangulated Möbius band $B_{N,M}$ for an instance of Möbius Sperner, the number of Sperner base triangles is odd. Finding one of them is in PPA.*

**Proof.** As Möbius Sperner has index 1, the oddness follows. The reduction to an AEUL is similar to that described earlier for the Möbius DPZP problem.   □

*Brouwer*

We define the Möbius version of Brouwer as follows:

**Definition 12** *(Möbius Brouwer($B_{N,M}, g; G$))*. The required input satisfies the same conditions as Möbius Sperner. The required output is a base square containing all three colors.

Similar to Möbius Sperner, we have

**Lemma 5.** *On any admissible triangulated Möbius band $B_{N,M}$ for an instance of Möbius Brouwer, the number of base squares containing all three colors is odd. Finding one of them is in PPA.*

*Simple Tucker*

We define the Möbius version of simple Tucker as follows:

**Definition 13** *(Simple Möbius Tucker($B_{N,M}, g; G$))*. Consider a triangulated Möbius grid $B_{N,M}$ and a polynomial-time machine $G$ that generates a function $g$ on $B_{N,M}$: $g(\mathbf{p}) = G(\mathbf{p}) \in \{\pm 1, \pm 2\}$, for any $\mathbf{p} \in B_{N,M}$. Further, we require $g(\cdot)$ to be Möbius feasible, i.e., $\forall y (-N \leq y \leq N)$, $g((N, y)) = g((-N, -y))$, and further to satisfy the special antipodal boundary condition defined as follows:

- $g((0, M)) = -2$; $g((0, -M)) = 2$
- $g((i, M)) = g((-i, -M)) = -1$, for every $i \in \mathbb{Z}$: $0 < i \leq N$
- $g((-i, M)) = g((i, -M)) = 1$, for every $i \in \mathbb{Z}$: $0 < i \leq N$

The required output is a complementary edge, defined as one with its two vertices colored as $+i$ and $-i$ for some $i \in \{1, 2\}$.

**Lemma 6.** *On a simple Möbius Tucker, there is always a complementary edge. Finding one is a problem belonging to the PPA class.*

**Proof.** Changing the colors $\{-1, -2\}$ of the vertices in Möbius Tucker into 0 reduces the problem to Möbius Sperner. As the boundary of the Möbius Sperner has index 1, there is always a fully colored base triangle $\delta$. The vertex colored 0 in $\delta$ was originally either $-1$ or $-2$ in the simple Möbius Tucker. Therefore, we obtain a complementary edge in the simple Möbius Tucker. The proof is complete. $\quad\square$

## 3. PPA-completeness of Möbius DPZP and its applications

We have already proven that Möbius DPZP is a problem belonging to the PPA class in the last section. We now prove the PPA-hardness of Möbius DPZP. For any instance input to $AEUL(T_n, C_n, 0^n)$, we construct a corresponding instance of Möbius DPZP in polynomial time so that each zero point in the Möbius DPZP instance maps back to another end node different from $0^n$ for some line in the input instance of AEUL($T_n, C_n, 0^n$). As the existence in the Möbius DPZP instance is guaranteed, the reduction finds a solution to the input instance $AEUL(T_n, C_n, 0^n)$. The PPA-hardness of Möbius DPZP follows.

Our construction will be divided into two main steps. First, we need to construct a planar AEUL. The input to an AEUL instance a polynomial circuit that provides an output consisting of three possibilities: nil, one node, or two nodes. We need to place those nodes on the plane so that the output nodes are next to the input node within a unit distance (along the x-coordinate or y-coordinate. Next we build a Möbius DPZP on top of the planar AEUL and color all the vertices so that each zero point will correspond to another end node of the original AEUL instance.

We emphasize here that when we say to color all the vertices or compute the neighbors of a node, we mean to develop a polynomial time algorithm to compute them whenever the input to the algorithm is given.

### 3.1. Extend to a planar AEUL instance

We start to embed a given AEUL($T_n, C_n, 0^n$) graph $G$ on the Möbius band.

Let the simple undirected graph $G = (V, E)$ of lines and cycles be the input instance of AEUL($T_n, C_n, 0^n$). Let $|V| = N = 2^n$.

We define $G^* = (V^*, E^*)$, where $V^* \subseteq B_{12N^2, 24N}$, and $E^* \subseteq \{(\mathbf{p}, \mathbf{p}') : \|\mathbf{p} - \mathbf{p}'\|_1 = 1, \mathbf{p}, \mathbf{p}' \in V^*\}$ to be defined as an embedding of $G = (V, E)$ on the plane in the following.

For every $\mathbf{p} \in V^*$, we define $K_{\mathbf{p}}$ by the base square having $\mathbf{p}$ at the bottom-left corner. That is, $V(K_{\mathbf{p}}) = \{\mathbf{q} : q_i \in \{p_i, p_i + 1\}, i = 1, 2\}$ and $E(K_{\mathbf{p}}) = E_{\mathbf{p}}^1 \cup E_{\mathbf{p}}^2$ where $E_{\mathbf{p}}^1 = \{(\mathbf{p}, \mathbf{p} + (0, 1)), (\mathbf{p} + (1, 0), \mathbf{p} + (1, 1))\}$, $E_{\mathbf{p}}^2 = \{(\mathbf{p}, \mathbf{p} + (1, 0)), (\mathbf{p} + (0, 1), \mathbf{p} + (1, 1))\}$. We also use the notations $|K_{\mathbf{p}} = \{(\mathbf{p}, \mathbf{p} + (1, 0)), (\mathbf{p}, \mathbf{p} + (0, 1))\}$, $\underline{K_{\mathbf{p}}}| = \{(\mathbf{p}, \mathbf{p} + (1, 0)), (\mathbf{p} + (1, 0), \mathbf{p} + (1, 1))\}$, $|\overline{K_{\mathbf{p}}} = \{(\mathbf{p}, \mathbf{p} + (0, 1)), (\mathbf{p} + (0, 1), \mathbf{p} + (1, 1))\}$, $\overline{K_{\mathbf{p}}}| = \{(\mathbf{p} + (0, 1), \mathbf{p} + (1, 1)), (\mathbf{p} + (1, 0), \mathbf{p} + (1, 1))\}$ to represent the corresponding edge sets.

For $\mathbf{p}, \mathbf{q} \in V^*$, if $p_i = q_i, i = 1$ or 2, let $\mathbf{u}^1, \mathbf{u}^2, \ldots, \mathbf{u}^m \in \mathbb{Z}^2$ be all the integer points on the (vertical or horizontal) segment $\mathbf{pq}$ which are labeled along $\mathbf{pq}$ with $\mathbf{u}^1 = \mathbf{p}$ and $\mathbf{u}^m = \mathbf{q}$. We say $K_{\mathbf{p}}$ and $K_{\mathbf{q}}$ are *connected* by a line segment. We denote them by $K_{\mathbf{p}}^i K_{\mathbf{q}}^i = \cup_{k=1}^m E_{\mathbf{u}^k}^i$ and place $\cup_{k=1}^m E_{\mathbf{u}^k}^i$ in $E^*$ for $i = 1, 2$. In case of no ambiguity, we simply write $K_{\mathbf{p}} K_{\mathbf{q}} = K_{\mathbf{p}}^i K_{\mathbf{q}}^i$ for $p_i = q_i$ to form a vertical or horizontal tunnel dependent on $i = 1$, or 2.

On the Möbius band, we also allow $K_{(12N^2-1, y)}^2$ and $K_{(-12N^2, -y-1)}^2, -24N \le y \le 24N - 1$ to be connected, that is, $E_{(12N^2-1, y)}^2 \cup E_{(-12N^2, -y-1)}^2 \subseteq E^*$.

Next, we define a connected path $K_{\mathbf{u}^1} K_{\mathbf{u}^m}$ for $\mathbf{u}^1, \mathbf{u}^2, \cdots, \mathbf{u}^m$ even in the case where they don't share the same x-coordinate nor y-coordinate. We do so by connecting them by a collection of connected line segments parallel to the two axes that turns into the appropriate directions at some intermediate points. Thus, when we connect $p = u^1$ and $q = u^m$ turning at point $u = \mathbf{u}^j$ toward the upper-right direction, we can construct the tunnel by edges on line segment $K_{\mathbf{p}}^1 K_{\mathbf{u}^{j-1}}^1$, $|\overline{K_{\mathbf{u}}}$ and line segment $K_{\mathbf{u}^{j+1}}^2 K_{\mathbf{q}}^2$. Similar connections can be constructed for other turns of $\pm 90$ degrees.

We are going to build $G^*$ as a planar embedded graph correspondent to the input graph $G$ for AEUL with nodes $\{0, 1, \ldots, N - 1\}$. The goal of the reduction is to keep the set of degree one nodes in $G^*$ the same as in the input graph $G$.

In order to further embed the graph $G^*$ into the DPZP problem, we will, for each edge of G, two paths in $G^*$ with a pair of parallel edges of distance one apart for each edge of $G$.

The graph $G$ will be of exponential in its size where $n$ is the input size of the polynomial size circuit $T_n$. We also construct a polynomial size circuit $T_n^*$ for $G^*$ which outputs two neighbors (or one, or none), for any given node.

To map nodes in $G$ to vertices in $G^*$, for every $i : 0 \le i < N$, node $i$ of $G$ maps to a vertex set $S_i = \cup_{k=24i}^{24i+11} \{K_{(0,k)}\}$. That is, we create a fixed-length "tube" $S_i$ for node $i$ in $G$. We call it a vertex tube. Every such tube has two ends, called the *up* end and the *down* end, depending on their values of the second coordinates on $V^*$, denoted by $S_i^{up} = K_{(0,24i+11)}$ and $S_i^{down} = K_{(0,24i)}$. The embedding of the starting node $\mathbf{0}^n$ is different from other nodes. For $i = 0$, we set $S_0 = \cup_{k=-24N}^{11} \{K_{(0,k)}\}$ in $G^*$.

We construct an undirected path between one of $\{S_i^{up}, S_i^{down}\}$ and one of $\{S_j^{up}, S_j^{down}\}$ if and only if edge $ij$ appears in $G$. Let $ij \in E$ and $ik \in E$ be the two edges connected to $j$ and $k$ from $i$. If $j > k$ we call $j$ the bigger neighbor and $k$ the smaller neighbor of the node $i$.

For each vertex tube, we connect its up end to its bigger neighbor (if the degree of the node is 1, we also take it to be the bigger one), and its down end to the smaller neighbor (if any).
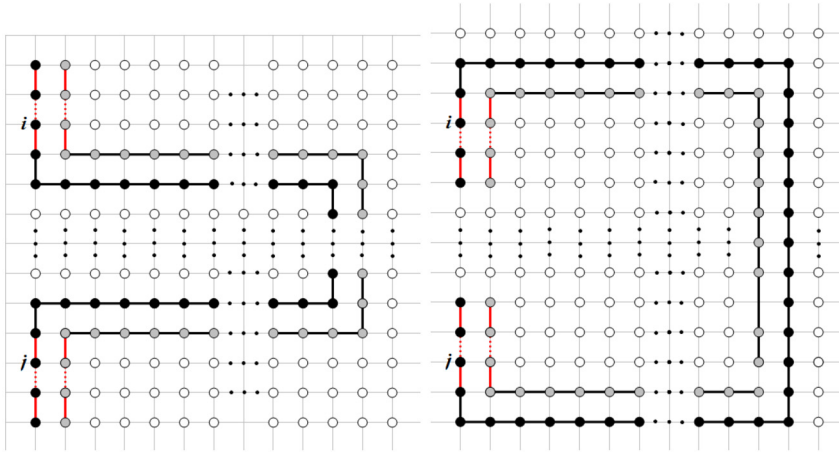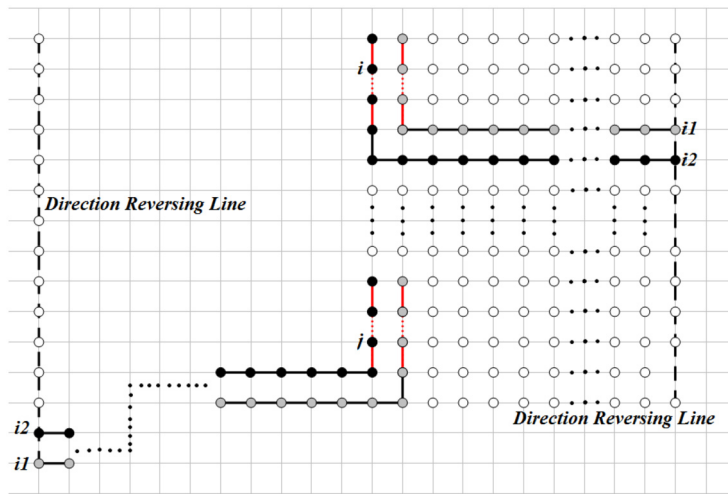
**Fig. 1.** Connecting Case 1.



**Fig. 2.** Connecting Case 2.

If $(i, j)$ is an edge in $G$, let $y_i, y_j$ be the y-coordinates of the ends of tube $i$ and $j$ which need to be linked together. Let $t = 12(N \cdot \max\{i, j\} + \min\{i, j\})$. We consider two different connection cases:

1. $S_i^{up} - S_j^{down}$ or $S_i^{down} - S_j^{up}$: we add edges $K_{(0, y_i)} K_{(t, y_i)}$, $K_{(t, y_i)} K_{(t, y_j)}$, $K_{(t, y_j)} K_{(0, y_j)}$ to $E^*$.
2. $S_i^{up} - S_j^{up}$ or $S_i^{down} - S_j^{down}$: without loss of generality, we assume that $i < j$. We add these edges $K_{(0, y_i)} K_{(12N^2 - 1, y_i)}$, $K_{(12N^2 - 1, y_i)} K_{(-12N^2, -y_i - 1)}$, $K_{(-12N^2, -y_i - 1)} K_{(-t - 1, -y_i - 1)}$, $K_{(-t - 1, -y_i - 1)} K_{(-t - 1, y_j)}$ and $K_{(-t - 1, y_j)} K_{(0, y_j)}$ to $E^*$.

Case 1 is a typical case as illustrated in Fig. 1. Case 2 is atypical and is involved with the Möbius band structure $B_{12N^2, 24N}$, which is illustrated in Fig. 2. For example, consider the case where the degree of $i$ is 2, i.e. $T(n, i) = \langle j, k \rangle, k > i, j$. We assume that $i > j$ and $T(n, j) = \langle k, i \rangle$. Let $t = 10(n \cdot i + j)$. We can link $S_i^{down}$ and $S_j^{down}$ by adding $K_{(0, 24i)} K_{(12N^2 - 1, 24i)}$, $K_{(12N^2 - 1, 24i)} K_{(-12N^2, -24i - 1)}$, $K_{(-12N^2, -24i - 1)} K_{(-t - 1, -24i - 1)}$, $K_{(-t - 1, -24i - 1)} K_{(-t - 1, 24j)}$, and $K_{(-t - 1, 24j)} K_{(0, 24j)}$ to $E^*$.

We should note that the planar embedding $G^*$ above for the AEUL graph $G$ is itself not yet one of degree no more than two. Two paths in $G^*$ implementing two edges in $G$ may intersect each other, such as for edges $(1, 3)$ and $(2, 4)$. We will have vertices of degree four. The key idea is to break such a vertex into two vertices of degree two with no intersection as shown in Fig. 3. We should discuss it in more details later, together with the vertex coloring steps.

### 3.2. Reduction to Möbius DPZP and other related non-orientable discrete fixed point computation

The remaining difficulties of the reduction are how to color the vertices of $G^*$, then extend the colors to the rest of vertices on $V_{12N^2, 24N}$ of Möbius DPZP to construct a feasible admissible instance of DPZP $(B_{N,M}, f)$. A special attention will be made to handle path crossing on the plane.
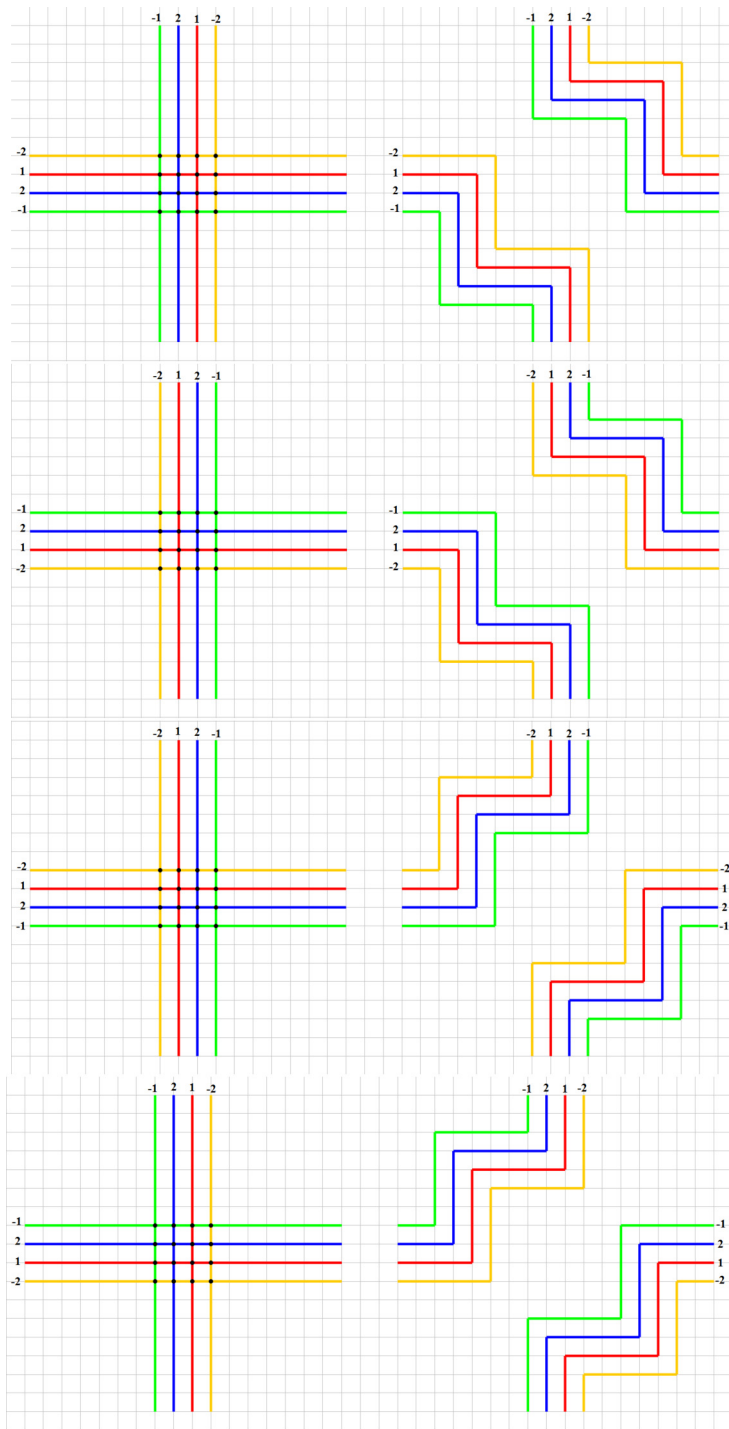
**Fig. 3.** Connection crossing.

**Lemma 7.** *Möbius DPZP is PPA-hard.*

**Proof.** Using the main structure $G^*$ above, we show how to design its coloring $f$. Then we extend $f$ to $B_{12N^2,24N}$ so that for any zero point of the Möbius DPZP, we can obtain a corresponding solution for the search problem AEUL.

The circuit $T_n$ of AEUL generates an undirected graph $G = (C_n, E)$, where $C_n = \{0, 1\}^n$. An edge $(u, v)$ appears in $E$ if and only if $u \in T_n(v)$ and $v \in T_n(u)$.

So given any $G$, we construct an instance $(f, G^*)$ on $V^* \subseteq V_{12N^2,24N}$ by the input circuit of $T_n$. It is applied to identify edges connecting a node to another and the degree one node of the AEUL graph. Such information can easily be used to construct $T^*$ to identify corresponding objects in $G^*$, in polynomial time.

We define the coloring function $f$ on $G^*$ and on $B_{12N^2,24N}$, as follows:

1. Color vertices on the boundary on $B_{12N^2,24N}$ according to the admissible conditions (recall Definition 9).
2. Color the long vertex tube: for $\forall j : -24N \leq j < 12$, set $f((0, j)) = 2$ and $f((1, j)) = 1$, which is a long vertex tube for the given node **0** of degree one.
3. Color the immediate neighbors of the long vertex tube with negative colors to make sure DPZP conditions hold along the internal part of the path: for $\forall j : -24N \leq j < 12$, set $f((-1, j)) = -1$ and $f((2, j)) = -2$.
4. Color the other vertex tubes: for $\forall i : 0 < i < N$, set $f((0, 24i + k)) = 2$ and $f((1, 24i + k)) = 1, k = 0, 1, 2, \ldots, 11$. We will need to modify the colors for the case of $k = 0$ later.
5. Color the immediate neighbors of the other vertex tubes with negative colors to make sure DPZP conditions hold along the internal part of the path: for $\forall i : 0 < i < N$: set $f((-1, 24i + k)) = -1$ and $f((2, 24i + k)) = -2, k = 0, 1, 2, \ldots, 11$.
6. Keep direction preserving conditions on ends of lines: For each leaf node $i : 0 < i < N$, we set their colors zero: $f(0, 24i) = f(1, 24i) = 0$.
7. Build an edge path: given an edge $(i, j) \in E$, w.l.o.g., assume that $i < j$, construct a path between $i$ and $j$ in $G^*$. Let $(i', j) \in E$ and $(i, j') \in E$. If $j > j'$, then the upper end of the tube for $i$ is connected to that for $j$. Otherwise, the lower end of the tube for $i$ is connected to that for $j$. Therefore, four possibilities exist.
   (a) $i > i'$ and $j < j'$: the lower end of the vertex tube for $i$ is connected to the upper end of the vertex tube for $j$ (see Fig. 1).
   (b) $i < i'$ and $j > j'$: the upper end of the vertex tube for $i$ is connected to the lower end of the vertex tube for $j$ (see Fig. 1).
   (c) $i < i'$ and $j < j'$: the lower end of the vertex tube for $i$ is connected to the lower end of the vertex tube for $j$ (see Fig. 2).
   (d) $i > i'$ and $j > j'$: the upper end of the vertex tube for $i$ is connected to the upper end of the vertex tube for $j$, similar to item (c).
8. Fill in the rest of the interior vertices with color $-2$.

Comments: Further adjustments should be made so that the colorings consistently link two vertex tubes.

1. We need parallel paths of width 4, making the colors crossing it to be a tuple $\langle -1, 2, 1, -2 \rangle$ (or $\langle -2, 1, 2, -1 \rangle$, depending on the direction we are moving) to maintain the direction preserving conditions. The vertex tubes for $i$ and $j$ connected in the four ways specified above will maintain it, that their colorings are consistent.
2. Note that if the path crosses the direction-reversing line, it must satisfy the Möbius condition, that is, the four vertices crossing the path must reverse their colors from $\langle -1, 2, 1, -2 \rangle$ to $\langle -2, 1, 2, -1 \rangle$ (or vice versa) after crossing the direction-reversing boundary.

The colorings along the parallel paths satisfy our condition of direction-preserving, as well as feasibility and admissibility conditions, except when two paths cross. We resolve this problem in the same way as [15] did. As shown in Fig. 3, all the changes are local and can be decided using the local information with a constant bounded number of function calls to the circuit $T$. We have thus provided the admissible coloring function which, given any point in $B_{12N^2,24N}$, provides its coloring in polynomial time using the polynomial time circuit $T$.

Note that nodes of color 0 in $G^*$ only appear in the mapping from $G$ to $G^*$ from a node of degree one in $G$. Therefore, finding a vertex of color 0 in $G^*$ is equivalent to finding the AEUL solution in $G$.

Hence we have proven that Möbius DPZP is PPA-hard.  □

We can now conclude that Möbius DPZP and simple Möbius Tucker are PPA-complete.

**Theorem 1.** *Möbius DPZP is PPA-complete.*

**Proof.** By Lemma 3, Möbius DPZP is in PPA. By Lemma 7, Möbius DPZP is PPA-hard. The proof is complete.  □

**Theorem 2.** *Simple Möbius Tucker is PPA-complete.*

**Proof.** Simple Möbius Tucker is in PPA by Lemma 6.

For PPA-hardness, we use the same construction as that in the proof of Lemma 7, except that this time the vertices colored 0 are colored $-2$. Therefore, at each vertex of color 0 in Lemma 7, we have an edge of color $+2$ and $-2$, and vice versa. The reduction follows. The proof is complete.  □

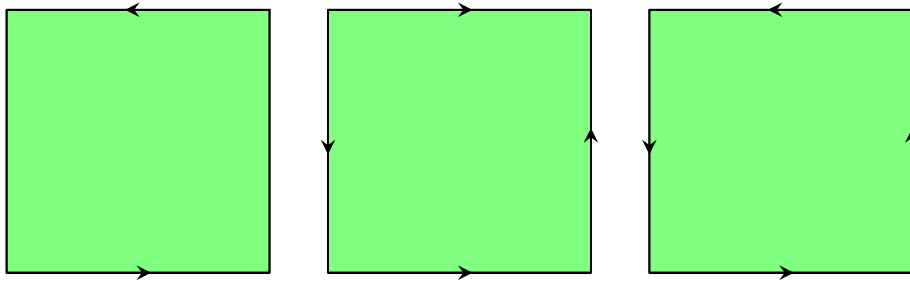Finally we show that Möbius Sperner and Möbius Brouwer are PPA-complete.

**Fig. 4.** Grid views: (a) Möbius band, (b) Klein bottle, (c) projective plane.

**Theorem 3.** *Möbius Sperner is PPA-complete.*

**Proof.** First, Möbius Sperner is in PPA by Lemma 4.

To prove that it is PPA-hard, we simply replace the colors of vertices colored $\{-1, -2\}$ to color 0 in the instance constructed in the PPA-hardness proof of Möbius DPZP. Finding a fully colored triangle $\delta$ in the instance of Möbius Sperner implies a true zero point in the instance of Möbius DPZP because the direction-preserving condition for Möbius DPZP, i.e. Definition 7, prevents another vertex in the same base triangle of color $\in \{-1, -2\}$. The proof is complete. □

**Theorem 4.** *Möbius Brouwer is PPA-complete.*

**Proof.** First, Möbius Brouwer is PPA-hard by Theorem 3. In the proof of the PPA-hard of Möbius Sperner, any path from one $(1, 2)$ edge to another crosses all the base squares on the path and ends at a base square containing only one base triangle.

The proof of Möbius Brouwer in PPA can be done by a reduction to Möbius Sperner. We split each base square of Möbius Brouwer in two, by choosing the diagonal in the standard triangulation. Then, the result follows. □

## 4. Discrete fixed points in projective space and Klein bottle

The PPA-hardness results we have discussed above can be extended to other non-orientable spaces. One idea is to slice out a Möbius band from the more complicated non-orientable space and to color it properly. Then, reducing the problem of finding the desired solution on the Möbius band can be reduced to the target problem.

Two of the most interesting spaces are the projective space and the Klein bottle. In this section, we reduce Möbius DPZP to both the projective plane and the Klein bottle so as to prove its PPA-hardness on those spaces. Since both cases are locally 2D objects, it is easy to triangulate them and to develop a connection graph of the base triangles in cycles and paths.

We have discussed two types of discrete fixed point problems: finding one, and given one finding another, depending on the boundary conditions. As both the projective space and the Klein bottle are closed without a boundary, we consider the second type of discrete fixed point problems, i.e. given one finding another.

In what follows, we will select the Möbius DPZP problem on the closed 2D plane to study. The similar techniques apply to other types of discrete fixed point problems as in the above. We omit them here as the results are easily provable similarly.

A 2D projective plane can be obtained from the sphere of a 3D ball by identifying two points on the sphere sharing the same diameter of the 3D ball. In other words, the two points $(x, y, z)$ and $(-x, -y, -z)$ in $S = \{(x, y, z) : x^2 + y^2 + z^2 = 1\}$ are merged into one point. We may focus on the semi-sphere $S^+ = \{(x, y, z) \in M : z \geq 0\}$. Note that all interior points in $S^+$ are independent, except the boundary points in $S^0 = \{(x, y, z) \in M : z = 0\}$, for which the two points $(x, y, 0)$ with $(-x, -y, 0)$ for $x^2 + y^2 = 1$ on the semisphere are identified with each other as in Fig. 4(c). This provides presentation of the projective DPZP that is most suitable for the proof that 2D Projective DPZP is in PPA.

**Definition 14** *(Projective 2D DPZP $(P_{N,M}, f)$)*. Given a triangulated Projective grid $P_{N,M}$ and a polynomial-time machine $F$ that generates a numeric direction-preserving function $f$ on $V_{N,M} : f(\mathbf{p}) \in \{0, \pm 1, \pm 2\}, \forall \mathbf{p} \in V_{N,M}$ with the boundary conditions as in Fig. 4(c) as well as an initial zero point base triangle Definition 8. The required output is another zero point base triangle (interior disjoint from the original one).

**Theorem 5.** *Given a triangulated projective plane labeled $\{0, \pm 1, \pm 2\}$ satisfying the DPZP property and an initial zero point base triangle, finding another zero point base triangle is a PPA-complete problem.*

**Proof.** To prove the problem in PPA, we construct an directed graph of paths and cycles, starting with the initial zero point base triangle as a node of degree one, two based triangle share an edge of the graph is they share an edge of color $1, 2$ in
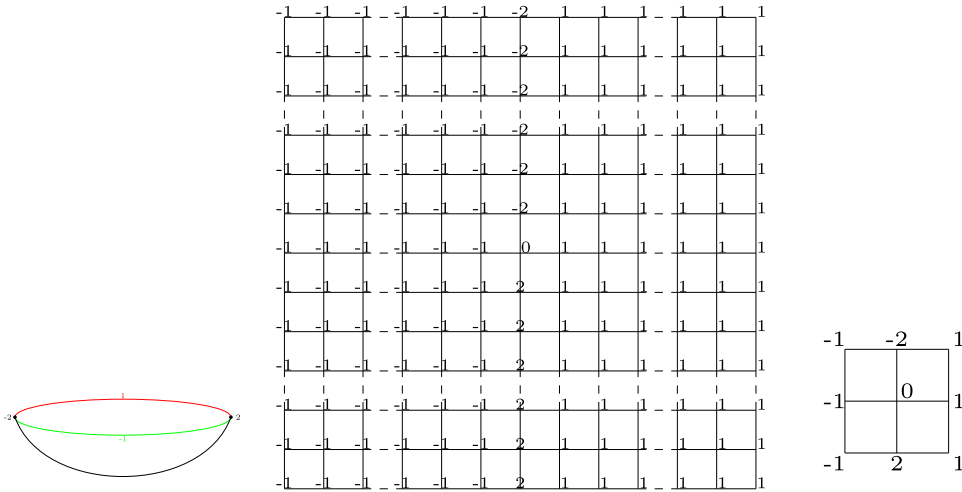
**Fig. 5.** Disk: (a) Its boundary view, (b) Coloring of vertices, (c) Simplified view.
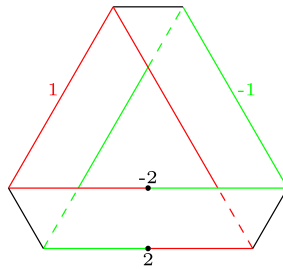


**Fig. 6.** The Möbius band boundary in red and green colors.

the Projective zero base triangle problem. To find another projective zero point base triangle, is clearly the edge of another line in the Projective zero point base triangle problem.

In the other direction of proof on PPA hardness, for any Möbius DPZP instance, we embed it in the projective plane to create a projective plane instance. We properly construct the projective plane instance so that there is a zero point base triangle and any other zero point base triangle will be one in the input Möbius DPZP instance.

As noted above, a 2D projective plane can be obtained from the sphere of a 3D unit ball by identifying two points sharing the same diameter. In other words, $(x, y, z)$ and $(-x, -y, -z)$ in $S = \{(x, y, z) : x^2 + y^2 + z^2 = 1\}$ are merged into one point. We can decompose $S$ into three pieces: $D^+ = \{(x, y, z) \in B : z \geq 1/2\}$ and $D^- = \{(x, y, z) \in B : z \leq -1/2\}$, as well as $M = \{(x, y, z) : |z| \leq 1/2 : (x, y, z) \in B\}$. In the projective space, $D^+$ and $D^-$ are the same disk centrally symmetric to each other by the bijection $(x, y, z) \leftrightarrow (-x, -y, -z)$. By the same projective bijection, $M$ is a centrosymmetric set. Hence $M$ can further be divided into two identical pieces, $M^+ = \{y \geq 0 : (x, y, z) \in M\}$ and $M^- = \{y \leq 0 : (x, y, z) \in M\}$, in the projective space. Further $M^+$ is a Möbius band, mapping $(x, 0, z) \in M$ to $(-x, 0, -z) \in M$ on its two opposing boundaries at the plane $y = 0$. And $M^-$ is the centrally symmetric image of $M^+$ with respect to $(0, 0, 0)$. so that they are the same in the projective space.

Now we are ready to embed any feasible admissible Möbius DPZP on the projective plane. We use such an input Möbius DPZP for $M^+$. We use the centrally symmetric image of $M^+$ for $M^-$. We use the admissible boundary condition in Definition to construct the boundary of the $D^+$ as in Fig. 5, the colors of which match those on the boundary of $M$ (Fig. 6) exactly. We color the disc as in Fig. 5(b), and at the center of the disk we place a zero point.

Note $D^+$ ($M^+$, respectively) and $D^-$ ($M^-$, respectively) are centrally symmetric to each other. Our problem in the projective space becomes that given one zero point base triangle in $D^+ \cup D^-$, find another in $M^+ \cup M^-$. A solution will be in $M^+$ (accompanied by its centrally symmetric image in $M^-$). As $M^+$ is a Möbius DPZP problem, that confirms the PPA-hard property of the projective space DPZP problem. $\square$

**Theorem 6.** *Given a triangulated Klein bottle labeled* $\{0, \pm 1, \pm 2\}$ *and a zero point base triangle, finding another zero point zero triangle is a PPA-complete problem.*

**Proof.** Similarly, the PPA completeness of the problem of finding another fixed point version extends naturally to the Klein bottle of [27]. Once again, the Klein bottle can only be embedded in the four-dimensional space.
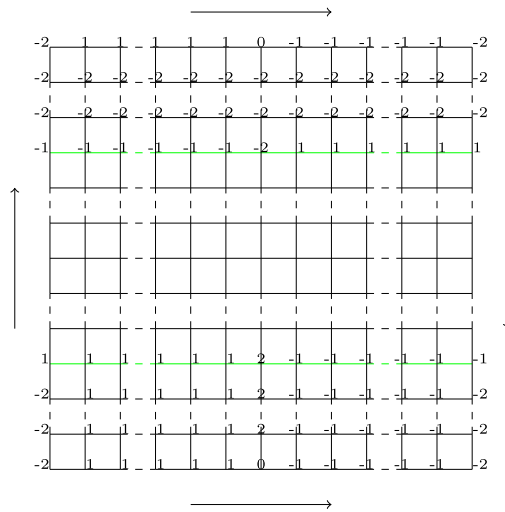
**Fig. 7.** Embedding DPZP in the Klein bottle.

We present a 2D view of it in Fig. 4(b) with slight modifications for ease of discussion. All three non-orientable 2D spaces are represented uniformly in the 2D grid, with their boundaries merged with the opposite sides.

Fig. 7 presents the embedding the DPZP grid in a Klein bottle Fig. 4(b). We triangulate each base squares in a 45 degree slant line segment to obtain a base triangle in each base square. There is a zero point base triangle at the middle bottom Fig. 7. Then we merge the top line and the bottom line along the arrow direction. The top and bottom zero points are merged into one in the Klein Bottle.

We aim to find another zero point base triangle on the Klein bottle constructed from this grid. If we remove the top four lines and the bottom four lines, we obtain a Möbius DPZP on the Möbius band only where another zero point base triangle could be hidden (its existence known by the property of Möbius DPZP.)

Therefore, given the bottom zero point base triangle, finding another one involves finding a zero point base triangle in the Möbius DPZP on the Möbius band embedded in the middle rows. □

## 5. High-dimensional non-orientable discrete fixed points

We have now proved that 2D fixed point problems on the Möbius band are PPA-complete, and so for other non-orientable spaces. In this section, we consider the generalized problem in a higher dimensional space with all constant side lengths. The proof is motivated by [4]. To handle the non-orientable space, we make key changes to the snake lemma to arrive at a dicephalic version of it. Considerable changes and new ideas are required. In the interest of space, we present the construction for one version of the discrete fixed points and the related proofs.

### 5.1. Uniform color boundary on the Möbius band

We introduce a special 2D Möbius band here for which the boundary consists of vertices all of the same color. Every instance of the problem has index 0. This naturally leads to a version of the fixed point problem where one fixed point is given and another needs to be found. We call such a case the uniform boundary coloring.

More precisely, the coloring function $f$ on a *uniform color boundary* Möbius band $B_{N,M}$ satisfies that: (1) $f((x, \pm M)) = 0, \forall x \in \mathbb{Z}, -N \le x \le N$; and (2) the Möbius condition, i.e. $f((N, y)) = f((-N, -y)), \forall y \in \mathbb{Z}, -M \le y \le M$. Then the Sperner problem on a uniform color boundary Möbius band can be defined as follows.

**Definition 15** (*Uniform-Color-Boundary Möbius Sperner*). Consider a triangulated Möbius grid $B_{N,M}$ and a polynomial-time machine $F$, which generates a function $f: f(\mathbf{p}) = F(\mathbf{p}) \in \{0, 1, 2\}, \forall \mathbf{p} \in B_{N,M}$. The Uniform-Color-Boundary Möbius Sperner conditions are as follows:

- $F((0, M - 1)) = 0; \ F((0, -M + 1)) = 2$
- $F((i, M - 1)) = F((-i, -M + 1)) = 0$, for every $i \in \mathbb{Z}: 0 < i \le N$
- $F((-i, M - 1)) = F((i, -M + 1)) = 1$, for every $i \in \mathbb{Z}: 0 < i \le N$
- Uniform Boundary Color: $F((i, -M)) = 0, \forall i \in \mathbb{Z}: |i| \le N$

$\{(0, -M + 1), (1, -M + 1), (0, -M)\}$ is the input base Sperner triangle, referring to base triangle containing all three colors $\{0, 1, 2\}$. The required output is another **Sperner base triangles**. In general, a fully colored base simplex is called a **Sperner base simplex**

Note that $index(B_{N,M}, f)$ is zero for a color function of the uniform color boundary Möbius band. According to Lemma 1, we have the following lemma:

**Lemma 8.** *For any uniform color boundary three-coloring of the triangulated Möbius band $B_{N,M}$, the number of Sperner base triangles is even. Given one Sperner base triangle, finding another one is a PPA-complete problem.*

**Proof.** Clearly, the index of any instance is 0. Therefore, there is an even number of fully colored base triangles. Given one fully colored Sperner base triangle, the existence of another is guaranteed.

The problem is in PPA because the relationship of two edges on a base triangle of colors (1,2) still holds and the uniform color boundary condition prevents the paths of the underlying AEUL from crossing the boundary.

In the other direction, Definition 15 has reduced Möbius Sperner to Uniform-Color-Boundary Möbius Sperner by adding an extra layer of vertices outside of the boundary and coloring them all 0. For an instance of Uniform-Color-Boundary Möbius Sperner, $(\{(0, -M - 1), (0, -M), (1, -M)\})$ is the given base Sperner triangle. Our goal becomes to find another Sperner base triangle for the original Möbius Sperner instance. $\square$

### 5.2. High-dimensional Möbius Sperner

We extend the 2D Uniform-Color-Boundary Möbius Sperner proven PPA-complete to higher dimensions. First we define the well-behaved function.

**Definition 16** *(Well-behaved function [4])*. A polynomial-time computable integer function $f$ is *well behaved*, if $\exists n_0 > 0 \ni \forall n \geq n_0$, $3 \leq f(n) \leq n/2$.

Define $K_{\mathbf{p}} = \{\mathbf{q} \in \mathbb{Z}^d \mid q_i = p_i \text{ or } p_i + 1, \forall 1 \leq i \leq d\}$.
For a positive integer $d$ and a vector $\mathbf{r} \in \mathbb{Z}^d$, let

$$A_{\mathbf{r}}^d = \left\{\mathbf{p} \in \mathbb{Z}^d \mid -r_i \leq p_i \leq r_i, \forall 1 \leq i \leq d\right\}$$

be the *hypergrid* with side length $\mathbf{r}$ (NOTE: $2r_i$ length in the $i$-th dimension because of the symmetry). In defining the boundary, we leave one dimension of the *boundary* of the hypergrid $\partial A_{\mathbf{r}}^d = \{\mathbf{p} \in A_{\mathbf{r}}^d \mid p_i = \pm r_i, \exists 2 \leq i \leq d\}$ open, to be merged to form the reversing subspace for the non-orientable property.

**Definition 17** *(The valid boundary condition)*. A coloring function $F : A_{\mathbf{r}}^d \to \{0, 1, \ldots, d\}$ is *valid* on $A_{\mathbf{r}}^d$ if the following boundary conditions hold:

1. (Uniform color boundary) For any $\mathbf{p} \in \partial A_r^d$, $F(\mathbf{p}) = 0$.
2. (Reversing face consistency) $\forall x_i, i = 2, 3, \ldots, d, F((r_1, x_2, x_3, \ldots, x_d)) = F((-r_1, -x_2, x_3, \ldots, x_d))$. Note that this is equivalent to merging $(r_1, x_2, x_3, \cdots, x_d)$ and $(-r_1, -x_2, x_3, \cdots, x_d)$ into one vertex.

The set of points $\{(\pm r_1, x_2, \ldots, x_d) : -r_i \leq x_i \leq r_i, i = 2, 3, \ldots, d\}$ are called *reversing face*. We include condition 2 here to guarantee the consistency of function values in the non-orientable space. Fixing other variables, $x_3, x_4, \cdots, x_d$ yields a *reversing plane* for the variables $x_1$ and $x_2$.

For any well-behaved function $f$, we define a corresponding Möbius Sperner fixed point problem as follows.

**Definition 18** *(Möbius Sperner$^f$)*. For a well-behaved function $f$ and a parameter $n$, let $m = f(n)$ and $d = \lceil n/f(n) \rceil$. An input instance of Möbius Sperner$^f$ is a pair $(F, 0^n)$, where $F$ is a valid coloring function with parameter $d$ and $\mathbf{r}$, where $r_i = 2^m, \forall i : 1 \leq i \leq d$. Given a point $\mathbf{p} \in A_{\mathbf{r}}^d$ where $K_{\mathbf{p}}$ is of index one, i.e., contains one base Sperner simplex in its triangulation, the output of this problem is another base Sperner simplex.

We have the following theorem.

**Theorem 7.** *For any well-behaved function $f$, Möbius Sperner$^f$ is PPA-complete.*

One can show that this problem is in PPA. To prove the hardness, similar to the orientable space in [4], we embed an instance of 2D Möbius Sperner(Möbius Sperner$^{f_2}$), which is known to be PPA-complete, in a space that is one dimension higher iteratively until Möbius Sperner$^f$. We show that the process for any local information can be obtained in a polynomial number of state transformations back to the 2D case. The details are presented in subsequent subsections.

### 5.2.1. Three technical lemmas

Triple $T = (F, d, \mathbf{r})$ represents a valid coloring function $F$ in the form of a Boolean circuit, implementing a valid coloring function with the dimension parameter $d$ and size vector $\mathbf{r} \in \mathbb{Z}^d$, $\forall\, i : 1 \leq i \leq d\ r_i \geq 3$. We restrict our discussion on case, where a panchromatic simplex P of T is given as the single panchromatic simplex in a unit hypercube.

Let Size$[F]$ denote the number of gates plus the number of input and output variables for function $F$. The embedding is achieved through a sequence of three polynomial-time transformations: $\mathbf{L}^1(T, t, u)$, $\mathbf{L}^2(T, u)$, and $\mathbf{L}^3(T, t, a, b)$. $\mathbf{L}^1(T, t, u)$ increases the size of the $t$-th dimension of the hypergrid from $r_t$ to $u$ (requiring $u > r_t$). $\mathbf{L}^2(T, u)$ extends the coloring to a space one dimension higher. $\mathbf{L}^3(T, t, a, b)$ folds a Möbius grid $T$ to $T'$ so that one more side length in a certain dimension is reduced to a constant size. At the same time, *from every Sperner simplex of $T'$, one can find a Sperner simplex of $T$ efficiently.* We use $\mathbf{e}_i$ as the vector for the $i$-th coordinate.

**Lemma 9** ($\mathbf{L}^1(T, t, u)$: *Padding a Dimension*). *Given a triple $T = (F, d, \mathbf{r})$ and two integers $1 \leq t \leq d$ and $u > r_t$, $\mathbf{L}^1(T, t, u)$ constructs a new coloring triple $T' = (F', d, \mathbf{r}')$ that satisfies the following two properties:*

**A.** *$r'_t = u$ and $r'_i = r_i\ i \in [d] \backslash \{t\}$. In addition, there exists a polynomial $g_1(n)$ such that Size$[F'] = $ Size$[F] + O(g_1(\text{Size}[\mathbf{r}']))$, and $F'$ can be computed in time polynomial in Size$[F']$. We write $T' = \mathbf{L}^1(T, t, u)$;*
**B.** *From each Sperner base simplex $P'$ of coloring triple $T'$, we can compute a Sperner base simplex $P$ of $T$ in polynomial time.*

**Proof.** Property **A** immediately by the algorithm in Algorithm 1. Property **B** follows since all new nodes added to $T'$ are the boundary nodes beyond $x_t > r_t$. As the boundary of $T$ is uniformly colored by 0, no Sperner base simplex can contain a new node in $T'$. The claim follows.  □

---

**Algorithm 1:** $\mathbf{L}^1(T, t, u)$: Padding a Dimension.

**Input:** $T = (F, d, \mathbf{r}), t, u$
**Output:** $(F', d, \mathbf{r}'), \mathbf{r}' = \mathbf{r} + (u - r_t)\mathbf{e}_t$
**1 if** $\mathbf{p} \in \partial A_{\mathbf{r}'}^d$ **then**
**2**  |  $F'(\mathbf{p}) = 0$;
**3 else if** $\mathbf{p} \in \partial A_{\mathbf{r}}^d$ **then**
**4**  |  $F'(\mathbf{p}) = F(\mathbf{p})$;
**5 else**
**6**  |  $F'(\mathbf{p}) = 0$.
**7 end**

---

**Lemma 10** ($\mathbf{L}^2(T, u)$: *Adding a Dimension*). *Given a coloring triple $T = (F, d, \mathbf{r})$ and an integer $u \geq 3$, $\mathbf{L}^2(T, u)$ constructs a new coloring triple $T' = (F', d + 1, \mathbf{r}')$ satisfying the following properties:*

**A.** *$r'_{d+1} = u$ and $r'_i = r_i$ for all $i \in [d]$. Moreover, there exists a polynomial $g_2(n)$ such that Size$[F'] = $ Size$[F] + O(g_2(\text{Size}[\mathbf{r}']))$. $F'$ can be computed in time polynomial in Size$[F']$. We write $T' = \mathbf{L}^2(T, u)$;*
**B.** *From each Sperner simplex $P'$ in the coloring triple $T'$, we can compute a Sperner simplex $P$ of $T$ in polynomial time.*

---

**Algorithm 2:** $\mathbf{L}^2(T, u)$: Adding a Dimension.

**Input:** $T = (F, d, \mathbf{r}), u$
**Output:** $T' = (F', d + 1, \mathbf{r}'), r'_{d+1} = u, (\forall i : 1 \leq i \leq d) r'_i = r_i$
**1 if** $\mathbf{p} \in \partial A_{\mathbf{r}'}^{d+1}$ **then**
**2**  |  $F'(\mathbf{p}) = 0$
**3 else if** $p_{d+1} = 1$ **then**
**4**  |  $F'(\mathbf{p}) = F(\widehat{\mathbf{p}})$ where $\widehat{\mathbf{p}} \in \mathbb{Z}^d$ satisfying $\widehat{p}_i = p_i$ for all $1 \leq i \leq d$;
**5 else if** $p_{d+1} = 0$ **then**
**6**  |  $F'(\mathbf{p}) = d + 1$;
**7 else**
**8**  |  $F'(\mathbf{p}) = 0$;
**9 end**

**Proof.** For each point $\mathbf{p} \in A^{d+1}_{\mathbf{r}'}$, we use $\widehat{\mathbf{p}}$ to denote the point $\mathbf{z} \in A^d_{\mathbf{r}}$ with $z_i = p_i$, $\forall i \in [d]$. The color assignment of $F'$ is given in Algorithm 2. Clearly, Property **A** is true.

To prove Property **B**, we let $P' \subset K_p$ be a Sperner simplex of $T'$. We note that $p_{d+1} = 0$. Otherwise, $K_p$ contains color $d + 1$ only if $p_{d+1} = -1$, in which case it only contains colors $d + 1$ and 0, a contradiction. Therefore, the Sperner simplex $P'$ must be in $K_p$ for $p_{d+1} = 0$. The remaining vertices, those in $\widehat{\mathbf{p}}$, must all be in $K_p$, which contains all the colors except $d + 1$, is therefore a Sperner simplex of $T$. $\square$

---

**Algorithm 3:** $\mathbf{L}^3(T, t, a, b)$: extends the coloring triple $T = (F, d, \mathbf{r})$.

**Input:** $T = (F, d, \mathbf{r}), a, b, t : 1 \le t \le d, r_t = a(2b + 1) + 5, a, b \ge 1$.
**Output:** $T' = (F', d + 1, \mathbf{r}'), r'_t = a + 5, r'_{d+1} = 4b + 3, (\forall i \ne t, 1 \le i \le d) \ r'_i = r_i$.

1 **if** $\mathbf{p} \in W$ **then**
2    |   $F'(\mathbf{p}) = F(\psi(\mathbf{p}))$
3 **else if** $\mathbf{p} \in \partial A^{d+1}_{\mathbf{r}'}$ **then**
4    |   $F'(\mathbf{p}) = 0$;
5 **else if** $p_{d+1} = 0$ **then**
6    |   $F'(\mathbf{p}) = d + 1$;
7 **else if** $p_{d+1} = 4i$ where $1 \le i \le b$ and $0 \le |p_t| \le a + 1$ **then**
8    |   $F'(\mathbf{p}) = d + 1$;
9 **else if** $p_{d+1} = 4i + 1, 4i + 2$ or $4i + 3$ where $0 \le i \le b - 1$ and $|p_t| \le 1$ **then**
10   |   $F'(\mathbf{p}) = d + 1$
11 **else**
12   |   $F'(\mathbf{p}) = 0$;
13 **end**

---

**Lemma 11** ($\mathbf{L}^3(T, t, a, b)$: dicephalic snake embedding). *Given a coloring triple $T = (F, d, \mathbf{r})$ and an integer $t : 1 \le t \le d$, if $r_t = a(2b + 1) + 5$ for two integers $a, b \ge 1$, then $\mathbf{L}^3$ constructs a new coloring triple $T' = (F', d + 1, \mathbf{r}')$ on the set $W$ defined by $r'_t = a + 5$, $r'_{d+1} = 4b + 3$, and $r'_i = r_i \ \forall i \in [d]\setminus\{t\}$.*

  **A.** *There exists a polynomial $g_3(n)$ such that $\text{Size}[F'] = \text{Size}[F] + O(g_3(\text{Size}[\mathbf{r}']))$ such that the value of $F'$ on $\mathbf{p} \in W$ can be identified to the value of $F$ on $\psi(\mathbf{p})$ in time polynomial in $\text{Size}[F']$. We write $T' = \mathbf{L}^3(T, t, a, b)$.*

  **B.** *From each Sperner simplex $P'$ of coloring triple $T'$, we can compute a Sperner simplex $P$ of $T$ in polynomial time.*

**Proof.** Consider the domains $A^d_{\mathbf{r}} \subset \mathbb{Z}^d$ and $A^{d+1}_{\mathbf{r}'} \subset \mathbb{Z}^{d+1}$ of our coloring triples. The reduction $\mathbf{L}^3(T, t, a, b)$ is carried out in three steps. We define a $d$-dimensional set $W \subset A^{d+1}_{\mathbf{r}'}$ that is large enough to contain $A^d_{\mathbf{r}}$. Then, we define a (many-to-one) map $\psi$ from $W$ to $A^d_{\mathbf{r}}$ that specifies an implicit embedding of $A^d_{\mathbf{r}}$ in $W$. Finally, we build a function $F'$ for $A^{d+1}_{\mathbf{r}'}$ and show that from each Sperner simplex of $T'$, a Sperner simplex of $T$ can be found in polynomial time.

A 2D view of $W \subset A^{d+1}_{\mathbf{r}'}$ is illustrated in Fig. 8. We use a (dicephalic) snake-pattern to realize the larger size in the $t$th dimension of $A^d_{\mathbf{r}}$ using the 2D space defined by a new smaller size $t$th dimension and another $(d + 1)$th dimension (of size much smaller by a multiplicative factor less than one) of $A^{d+1}_{\mathbf{r}'}$, to roughly maintain the condition $r_t = r'_t \times r'_{d+1}$ (in fact, $r_t = O(r'_t \times r'_{d+1})$). Formally, $W$ consists of points $\mathbf{p} \in A^{d+1}_{\mathbf{r}'}$ satisfying $1 \le p_{d+1} \le 4b + 1$ and

- if $p_{d+1} = 1$, then $2 \le p_t \le a + 4$ or $-(a + 4) \le p_t \le -2$;
- if $p_{d+1} = 4b + 1$, then $-(a + 2) \le p_t \le a + 2$;
- if $p_{d+1} = 4(b - i) - 1$ where $0 \le i \le b - 1$, then $2 \le p_t \le a + 2$ or $-(a + 2) \le p_t \le -2$;
- if $p_{d+1} = 4(b - i) - 3$ where $0 \le i \le b - 2$, then $2 \le p_t \le a + 2$ or $-(a + 2) \le p_t \le -2$;
- if $p_{d+1} = 4(b - i) - 2$ where $0 \le i \le b - 1$, then $p_t = 2$ or $-2$;
- if $p_{d+1} = 4(b - i)$ where $0 \le i \le b - 1$, then $p_t = a + 2$ or $-(a + 2)$.

To build $T'$, we embed the coloring triple $T$ in $W$. The embedding is implicitly given by a many-to-one mapping $\psi$ from $W$ to $A^d_{\mathbf{r}}$, which will play a vital role in the coloring and the analysis of our reduction. For each $\mathbf{p} \in W$, we use $\mathbf{p}[m]$ to denote the point $\mathbf{q}$ in $\mathbb{Z}^d$ with $q_t = m$ and $q_i = p_i$ for all other $i \in [d]$. We will use the sign function $sgn(x) = 1$ if $x > 0, -1$ if $x < 0$, $and\, 0$ if $x = 0$ to define $\psi(\mathbf{p})$ according to the following cases:

- if $p_{d+1} = 1$, then $\psi(\mathbf{p}) = \mathbf{p}[2ab \cdot sgn(p_t) + p_t]$;
- if $p_{d+1} = 4b + 1$, then $\psi(\mathbf{p}) = \mathbf{p}[p_t]$;
- if $p_{d+1} = 4(b - i) - 1$ where $0 \le i \le b - 1$, then $\psi(\mathbf{p}) = \mathbf{p}[((2i + 2)a + 4) \cdot sgn(p_t) - p_t]$;
- if $p_{d+1} = 4(b - i) - 3$ where $0 \le i \le b - 2$, then $\psi(\mathbf{p}) = \mathbf{p}[(2i + 2)a \cdot sgn(p_t) + p_t]$;
- if $p_{d+1} = 4(b - i) - 2$ where $0 \le i \le b - 1$, then $\psi(\mathbf{p}) = \mathbf{p}[((2i + 2)a + 2) \cdot sgn(p_t)]$;
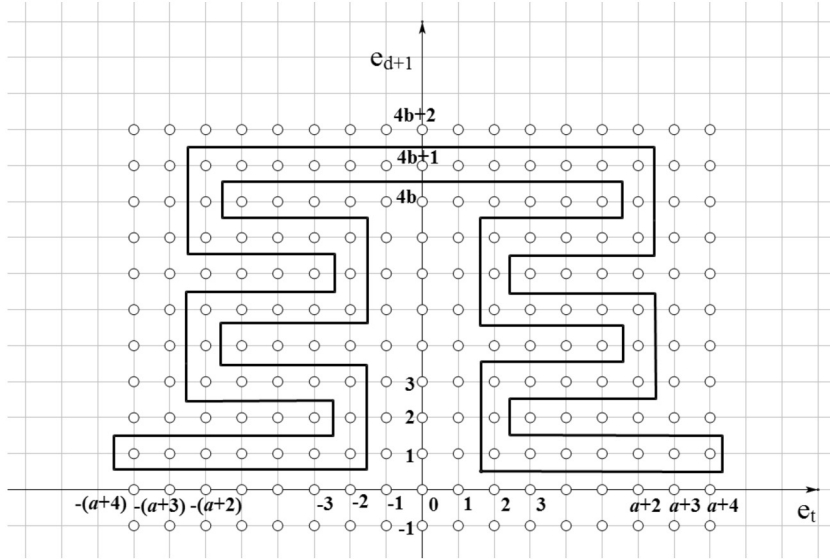
**Fig. 8.** A 2D view of set $W \subset A_{\mathbf{r}'}^{d+1}$.

- if $p_{d+1} = 4(b - i)$ where $0 \leq i \leq b - 1$, then $\psi(\mathbf{p}) = \mathbf{p}[((2i + 1)a + 2) \cdot sgn(p_t)]$.

We let $\psi_i(\mathbf{p})$ denote the $i$th component of $\psi(\mathbf{p})$.

**Proposition 1** (Valid *Boundary Condition Preserving*). *The coloring function $F'$ described in* Algorithm 3 *is valid on* $A_{\mathbf{r}'}^{d+1}$.

**Proof.** First we show that $F'$ satisfies the uniform color boundary condition (condition 1 of Definition 17) for all $\mathbf{p} \in \partial A_{\mathbf{r}'}^{d+1}$. We only need to prove that every vertex $\mathbf{p} \in W \cap \partial A_{\mathbf{r}'}^{d+1}$ is colored zero by step 2 of Algorithm 3.

$\forall \mathbf{p} \in W \cap \partial A_{\mathbf{r}'}^{d+1}$, by the definition of $\psi(\cdot)$, and therefore we have $p_i = \pm r_i'$ if and only if $\psi_i(\mathbf{p}) = \pm r_i$ for $(i : d \geq i \geq 2)$. It follows that $F'(\mathbf{p}) = F(\psi(\mathbf{p})) = 0$ by the valid boundary condition for $F$. Therefore, $F'$ satisfies the valid boundary condition (condition 1 of Definition 17).

Next we show that $F'$ satisfies the condition of reversing face consistency (condition 2 of Definition 17).

- If $t > 2$, then $F'$ obviously satisfies the condition of reversing face consistency, since neither $x_1$ nor $x_2$ is changed for the set of other variables.
- If $t = 1$, we consider two points $\mathbf{p} = (r_1', x_2, x_3, \ldots, x_d, x_{d+1})$ and $\mathbf{p}' = (-r_1', -x_2, x_3, \ldots, x_d, x_{d+1})$. If $x_{d+1} \neq 1$, $F'(\mathbf{p}) = F'(\mathbf{p}') = 0$. If $x_{d+1} = 1$, then $\mathbf{p}, \mathbf{p}' \in W$. Thus $F'(\mathbf{p}) = F(\psi(\mathbf{p}))$, $F'(\mathbf{p}') = F(\psi(\mathbf{p}'))$. Since $F$ is valid, $F(\psi(\mathbf{p})) = F(\psi(\mathbf{p}')))$ by definition of $\psi(\cdot)$. Therefore, $F'(\mathbf{p}) = F'(\mathbf{p}')$.
- If $t = 2$, we consider two points $\mathbf{p} = (r_1, x_2', x_3, \ldots, x_d, x_{d+1})$ and $\mathbf{p}' = (-r_1, -x_2', x_3, \ldots, x_d, x_{d+1})$. Because $\mathbf{p}$ and $\mathbf{p}'$ are centrally symmetric in the reversing plane, they are either both in or both not in $W$. If $\mathbf{p}, \mathbf{p}' \in W$, then $F'(\mathbf{p}) = F(\psi(\mathbf{p})) = F(\psi(\mathbf{p}')) = F'(\mathbf{p}')$ (since $F$ is valid). If $\mathbf{p}, \mathbf{p}'$ are not in $W$, we have $F'(\mathbf{p}) = F'(\mathbf{p}') = 0$ (where p is outside $W$ or $p_{d+1} < 0$) or $F'(\mathbf{p}) = F'(\mathbf{p}') = d + 1$ (where $p$ is inside $W$).

Therefore, $F'$ is a valid coloring function on $A_{\mathbf{r}'}^{d+1}$.  □

Clearly, whether $\mathbf{p} \in W$ or not can be decided in polynomial time by $\mathbf{L}^3$. Property **A** in Lemma 11 follows from the construction in Algorithm 3.

Next, we establish Property **B** of Lemma 11.

The intuition behind the proof is as follows. In $F'$, vertices to the inside of $W$ are colored $d + 1$, and vertices to the outside are colored 0. Every (unit-size) hypercube $K_{\mathbf{p}} \subset A_{\mathbf{r}'}^{d+1}$ consists of $K_{\mathbf{p}} \cap W$, whose image $\psi(K_{\mathbf{p}} \cap W)$ is a (unit-size) hypercube in $A_{\mathbf{r}}^d$, and vertices either to the inside or to the outside of $W$ but not both. Let $P'$ be a Sperner simplex of $T'$ in $A_{\mathbf{r}'}^{d+1}$. Let $K_{\mathbf{p}^*}$ be the hypercube containing $P'$. Since hypercubes to the outside of $W$ do not have a vertex of color $d + 1$, $K_{\mathbf{p}^*}$ must lie to the inside of $W$. We will show that, except the vertex of color $d + 1$, every vertex $\mathbf{p} \in P'$ either belongs to $W \cap K_{\mathbf{p}^*}$ or can be mapped to a vertex $\mathbf{q} \in W \cap K_{\mathbf{p}^*}$, such that $F'(\mathbf{q}) = F'(\mathbf{p})$. Thus from $P'$, we can recover $d + 1$ points in $W \cap K_{\mathbf{p}^*}$ with $d + 1$ distinct colors $\{0, 1, \ldots, d\}$. Since $F'(\mathbf{p}) = F(\psi(\mathbf{p}))$ for all $\mathbf{p} \in W$, we can apply $\psi$ to obtain a Sperner simplex $P$ of $T$.

We now proceed to formally prove a collection of claims to cover all possible cases of the given Sperner simplex $P'$ of $T'$. We use the following notation: for each $\mathbf{p} \in A_{\mathbf{r}'}^{d+1}$, let $\mathbf{p}[m_1, m_2]$ denote the vertex $\mathbf{q} \subset \mathbb{Z}^{d+1}$ such that $q_t = m_1$, $q_{d+1} = m_2$ and $q_i = p_i$ for all other $i \in [d]$.

**Claim 1.** If $p_t^* = 0$, then $p_{d+1}^* = 4b$. Furthermore, for every vertex $\mathbf{p} \in P'$ such that $F'(\mathbf{p}) \neq d+1$, $F(\psi(\mathbf{p}[p_t, 4b+1])) = F'(\mathbf{p})$.

**Proof.** For the first part of the claim, we have the following contradictions if $p_{d+1}^* \neq 4b$ and $p_t^* = 0$.

1. If $p_{d+1}^* = 4b + 1$, $K_{\mathbf{p}^*}$ does not contain color $d + 1$.
2. $p_{d+1}^* < 0$: $F'(\mathbf{p}) \in \{0, d+1\}$, the colors of vertices in $K_{\mathbf{p}^*}$ can only be 0 or $d + 1$.
3. $p_{d+1}^* < 4b$: $p_t^* = 0$ implies $p_t \in \{0, 1\}$. Therefore, each vertex $\mathbf{q} \in K_{\mathbf{p}^*}$ is colored according to one of the conditions in line 3, 4, 5 or 6 of Algorithm 3. For each $\mathbf{q} \in K_{\mathbf{p}^*}$, $F'(\mathbf{q}) = 0$ or $d+1$ from the procedure in Algorithm 3.

Then, $K_{\mathbf{p}^*}$ cannot be a Sperner hypercube, contradicting the assumption of the claim. Putting these cases together, we have $p_{d+1}^* = 4b$.

We now prove the second part of the claim. If $p_{d+1} = 4b + 1$, then the second part is proved because $F(\psi(\mathbf{p})) = F'(\mathbf{p})$ according to line 1 of Algorithm 3. Then $p_{d+1} = 4b$ is the only other possibility. Therefore, by the condition $F'(\mathbf{p}) \neq d+1$, according to line 2 and 4 of Algorithm 3, we have $\mathbf{p} \in W \cap \partial A_{\mathbf{r}'}^{d+1}$ and $\mathbf{p}[p_t, 4b+1] = \mathbf{p}$. We thus have $F(\psi(\mathbf{p}[p_t, 4b+1])) = F'(\mathbf{p}[p_t, 4b+1]) = F'(\mathbf{p})$, which completes the proof of the claim. $\square$

**Claim 2.** If $p_t^* = a + 2$ or $a + 3$, then $p_{d+1}^* = 0$. In addition, for each vertex $\mathbf{p} \in P'$ such that $F'(\mathbf{p}) \neq d+1$, $F(\psi(\mathbf{p}[p_t, 1])) = F'(\mathbf{p})$.

**Proof.** Obviously, $p_{d+1}^* \geq 0$. If $p_{d+1}^* > 0$, then $K_{\mathbf{p}^*}$ does not contain color $d + 1$, so we have $p_{d+1}^* = 0$. The first half of the claim holds.

For the second half of the claim, if $\mathbf{p} \in W$, the claim follows. We consider the following three cases:

- $p_{d+1} = 1$: then $\mathbf{p}$ is in $W$, and we have $F(\psi(\mathbf{p}[p_t, 1])) = F'(\mathbf{p})$.
- $\mathbf{p} \in A_{\mathbf{r}'}^{d+1} \setminus \partial A_{\mathbf{r}'}^{d+1}$: recall that $F'(\mathbf{q}) = d+1$ for all $\mathbf{q} \in A_{\mathbf{r}'}^{d+1} \setminus \partial A_{\mathbf{r}'}^{d+1}$ with $q_{d+1} = 0$, and we know that $p_t \in \{a+2, a+3, a+4\}$. Therefore $\mathbf{p}$ is also in $W$ in this case.
- $\mathbf{p} \in \partial A_{\mathbf{r}'}^{d+1}$: Recall $\mathbf{p}[p_t, 1] \in \partial A_{\mathbf{r}'}^{d+1}$, and $\psi(\mathbf{p}) = \psi(\mathbf{p}[p_t, 1])$, hence we have that $F(\psi(\mathbf{p}[p_t, 1])) = F(\psi(\mathbf{p})) = F'(\mathbf{p})$.

Combining these three cases, the second half of the claim follows. $\square$

**Claim 3.** If $p_{d+1}^* = 4b$, then $0 \leq p_t^* \leq a + 1$. Moreover, for each vertex $\mathbf{p} \in P'$ such that $F'(\mathbf{p}) \neq d+1$, $F(\psi(\mathbf{p}[p_t, 4b+1])) = F'(\mathbf{p})$.

**Proof.** If $p_t^* > a + 1$, then $K_{\mathbf{p}^*}$ does not contain color $d + 1$. Hence, $0 \leq p_t^* \leq a + 1$. Similar to the proof of Claim 1, we can prove the second part for the case when $0 \leq p_t \leq a + 1$.

When $p_t = a + 2$, both $\mathbf{p}$ and $\mathbf{p}[p_t, 4b+1]$ are in $W$, and we have $\psi(\mathbf{p}) = \psi(\mathbf{p}[p_t, 4b+1])$. Thus, $F(\psi(\mathbf{p}[p_t, 4b+1])) = F(\psi(\mathbf{p})) = F'(\mathbf{p})$. $\square$

We can similarly prove the following claims.

**Claim 4.** If $p_{d+1}^* = 4i + 1$ or $4i + 2$ for some $0 \leq i \leq b - 1$, then $p_t^* = 1$. Moreover, for each $\mathbf{p} \in P'$ such that $F'(\mathbf{p}) \neq d+1$, $F(\psi(\mathbf{p}[2, p_{d+1}])) = F'(\mathbf{p})$.

**Claim 5.** If $p_{d+1}^* = 4i$ for some $1 \leq i \leq b-1$, then $1 \leq p_t^* \leq a+1$. In addition, for each $\mathbf{p} \in P'$ such that $F'(\mathbf{p}) \neq d+1$, if $2 \leq p_t \leq a+1$, then $F(\psi(\mathbf{p}[p_t, 4i+1])) = F'(\mathbf{p})$; if $p_t = 1$, then $F(\psi(\mathbf{p}[2, 4i+1])) = F'(\mathbf{p})$.

**Claim 6.** If $p_{d+1}^* = 4i - 1$ for some $1 \leq i \leq b$, then $1 \leq p_t^* \leq a+1$. Moreover, for each $\mathbf{p} \in P'$ such that $F'(\mathbf{p}) \neq d+1$, if $2 \leq p_t \leq a+1$, then $F(\psi(\mathbf{p}[p_t, 4i-1])) = F'(\mathbf{p})$; if $p_t = 1$, then $F(\psi(\mathbf{p}[2, 4i-1])) = F'(\mathbf{p})$.

**Claim 7.** If $p_{d+1}^* = 0$, then $1 \leq p_t^* \leq a+3$. In addition, for each vertex $\mathbf{p} \in P'$ such that $F'(\mathbf{p}) \neq d+1$, if $2 \leq p_t^* \leq a+3$, then $\mathbf{p} \in W$ (and thus, $F(\psi(\mathbf{p})) = F'(\mathbf{p})$); if $p_t^* = 1$, then $F'(\psi(\mathbf{p}[2, 1])) = F'(\mathbf{p})$.

In addition,

**Claim 8.** $p_{d+1}^* \neq 4b + 1$.

---

**The Construction of $T^{3m'-14}$ from $T^1$**

---

1. **for any** $t$ from 0 to $m'-6$ **do**
2.     **let** $u = (2^{(m'-t-1)(l-2)} - 5)(2^{l-1} - 1) + 5$
3.     $T^{3t+2} = \mathbf{L}^1(T^{3t+1}, 1, u)$
4.     $T^{3t+3} = \mathbf{L}^3(T^{3t+2}, 1, 2^{(m'-t-1)(l-2)}, 2^{l-2} - 1)$
5.     $T^{3t+4} = \mathbf{L}^1(T^{3t+3}, t+3, 2^l)$

**Fig. 9.** The construction of $T^{3m'-14}$ from $T^1$.

---

**The Construction of $T^{w'}$ from $T^{3m'-14}$**

---

1. **let** $t = 0$
2. **while** $T^{3(m'+t)-14} = (C^{3(m'+t)-14}, m'+t-3, \mathbf{r}^{3(m'+t)-14})$ satisfies $r_1^{3(m'+t)-14} > 2^l$ **do**
3.     **let** $k = \lceil (r_1^{3(m'+t)-14} - 5)/(2^{l-1} - 1) \rceil + 5$
4.     $T^{3(m'+t)-13} = \mathbf{L}^1(T^{3(m'+t)-14}, 1, (k-5)(2^{l-1} - 1) + 5)$
5.     $T^{3(m'+t)-12} = \mathbf{L}^3(T^{3(m'+t)-13}, 1, k, 2^{l-2} - 1)$
6.     $T^{3(m'+t)-11} = \mathbf{L}^1(T^{3(m'+t)-12}, m'+t-2, 2^l)$, **set** $t = t+1$
7. **let** $w' = 3(m'+t) - 13$ and $T^{w'} = \mathbf{L}^1(T^{3(m'+t)-14}, 1, 2^l)$

**Fig. 10.** The construction of $T^{w'}$ from $T^{3m'-14}$.

**Proof.** If $p^*_{d+1} = 4b + 1$ then $K_{\mathbf{p}^*}$ does not contain color $d+1$. $\quad\square$

Here we do not list the cases where $p_t < 0$ as they are all the same as the above claims since $W$ is symmetric (technically, there is one unit-sized bias between the negative and positive cases about the $t$th dimension). Note that $p^*_{d+1} \geq 0$ in our construction of $T'$. Suppose that $P'$ is a Sperner simplex of $T'$, and $K_{\mathbf{p}^*}$ is the hypercube containing $P'$, then $P'$ and $\mathbf{p}^*$ must satisfy the conditions of one of the claims above. By that claim, we can transform every vertex $\mathbf{p} \in P'$, (aside from the one that has color $d+1$) back to a vertex $\mathbf{q}$ in $A_{\mathbf{r}}^d$ to obtain a set $P$ from $P'$. Since $P$ is accommodated, it is a Sperner simplex of $t$. Thus, with all the claims above, we can specify an efficient algorithm to compute a Sperner simplex $P$ of $T$ given a Sperner simplex $P'$ of $T'$. $\quad\square$

### 5.2.2. Proof of the PPA-hardness in Theorem 7

**Proof.** Starting with the 2D case, a folding process presented next changes the size of each dimension one by one to make the size in accordance to that of the well-behaved functions. Each step uses operations $\mathbf{L}^1(T, t, u)$, $\mathbf{L}^2(T, u)$, and $\mathbf{L}^3(T, t, a, b)$ to achieve this goal and maintains the validity of boundary conditions by Lemmas 9, 10 and 11.

The folding framework from [4] can be used in our version of the three basic operations, $\mathbf{L}^1$, $\mathbf{L}^2$ and $\mathbf{L}^3$, introduced above. We simplify the construction process as follows.

Formally, let $(F, 0^{2n})$ be an input instance of Möbius Sperner$^{f_2}$, already proven PPA-complete. Recall that $f_2(n) = \lfloor n/2 \rfloor$. Let

$$l = f(11n) \geq 3, m' = \left\lceil \frac{n}{l-2} \right\rceil, \text{ and } m = \left\lceil \frac{11n}{l} \right\rceil.$$

For any well-behaved function $f$, we reduce Möbius Sperner$^{f_2}$ to Möbius Sperner$^f$ by iteratively constructing a sequence of coloring triples $\mathcal{T} = \{T^0, T^1, \ldots, T^w\}$ for some $w = O(m)$, where $T_0 = (F, 2, (2^n, 2^n))$ and $T_w = (F^w, m, \mathbf{r}^w)$ such that $\mathbf{r}^w \in \mathbb{Z}^m$ and $\mathbf{r}_i^w = 2^l$ for any $i, 1 \leq i \leq m$. At each phase $t$, we employ one of the three technical lemmas $\mathbf{L}^1$, $\mathbf{L}^2$ and $\mathbf{L}^3$ described in the previous subsection with appropriate parameters to construct $T^{t+1}$ from $T^t$.

First, we invoke $\mathbf{L}^1\left(T^0, 1, 2^{m'(l-2)}\right)$ to obtain $T^1 = \left(C^1, 2, \left(2^{m'(l-2)}, 2^n\right)\right)$, for which the precondition of $\mathbf{L}^1$ holds as $m'(l-2) \geq n$. Next we call the procedure in Fig. 9. During each loop, the first component of $\mathbf{r}$ decreases by a factor of $2^{l-2}$ while the dimension of the space increases by 1 and the new dimension is of a size that satisfies the requirement. After this subprocess, we obtain a temporary coloring triple $T^{3m'-14} = \left(C^{3m'-14}, d^{3m'-14}, \mathbf{r}^{3m'-14}\right)$, such that

$$d^{3m'-14} = m' - 3, r_1^{3m'-14} = 2^{5(l-2)}, r_2^{3m'-14} = 2^n \text{ and } r_i^{3m'-14} = 2^l,$$

for any $i : 3 \leq i \leq m'-3$. Next, we invoke the procedure given in Fig. 10. Note that the while-loop must terminate in at most eight iterations because we started with $r_1^{3m'-14} = 2^{5(l-2)}$. The procedure returns a coloring triple $T^{w'} = \left(C^{w'}, d^{w'}, \mathbf{r}^{w'}\right)$ that satisfies

$$w' \leq 3m' + 11, d^{w'} \leq m' + 5, r_1^{w'} = 2^l, r_2^{w'} = 2^n, r_i^{w'} = 2^l, \text{ for any } i : 3 \leq i \leq d^{w'}.$$

Then we repeat the whole process above on the second coordinate and obtain a coloring triple $T^{w''} = \left( C^{w''}, d^{w''}, \mathbf{r}^{w''} \right)$, such that

$$w'' \leq 6m' + 21, d^{w''} \leq 2m' + 8 \text{ and } r_i^{w''} = 2^l, \text{ for any } i : 1 \leq i \leq d^{w''}.$$

Now following our initial definition for $m$ and $m'$, we have

$$d^{w''} \leq 2m' + 8 \leq 2\left( \frac{n}{l-2} + 1 \right) + 8 \leq 2\left( \frac{n}{l/3} \right) + 10 = \frac{6n}{l} + 10 \leq \frac{11n}{l} \leq m.$$

Finally, we repeatedly apply $\mathbf{L}^2$ for $m - d^{w''}$ times with parameter $u = 2^l$ to obtain the final coloring triple $T^w = (C^w, m, \mathbf{r}^w)$, where $r_i^w = 2^l$ for any $i, 1 \leq i \leq m$. Thus we obtain $w = O(m)$.

Now we prove that the whole construction is indeed a reduction from Möbius Sperner$^{f_2}$ to Möbius Sperner$^f$. Let $T^i = (C^i, d^i, \mathbf{r}^i)$. As sequence $\left\{ \text{Size} \left[ \mathbf{r}^i \right] \right\}_{0 \leq i \leq w}$ is non-decreasing and $w = O(m) = O(n)$, by Property **A** of Lemmas 9, 10 and 11, there exists a polynomial $g(n)$ such that $\text{Size} [C^w] = \text{Size} [C] + O(g(n))$. By Properties **A** of Lemmas 9, 10 and 11 again, we can construct the whole sequence $\mathcal{T}$ and in particular, $T^w = (C^w, m, \mathbf{r}^2)$, in time polynomial in $\text{Size} [C]$.

The pair $(C^w, 0^{11n})$ is an input instance of Möbius Sperner$^f$. Given a Sperner simplex $P$ of $(C^w, 0^{11n})$, using the algorithm in Property **B** of Lemmas 9, 10 and 11, we can compute a sequence of Sperner simplexes $P^w = P, P^{w-1}, \ldots, P^0$ iteratively in polynomial time, where $P^t$ is a Sperner simplex of $T^t$ and can be computed from the Sperner simplex $P^{t+1}$ of $T^{t+1}$. We can thus obtain $P^0$, which is a Sperner set of $(C, 0^{2n})$. $\square$

## 5.3. Alignment of adjacent base triangles via Kuhn triangulation

There is an issue of alignment on of triangulations on the boundary of two adjacent base triangles in the above PPA-complete proof using the two headed snake embedding.[1]

Issue 1  Given a $(d+1)$-dim panchromatic simplex P, After removing the vertex in P with color $d+1$, the other d vertices lie in W and can be mapped back to a panchromatic simplex in the original d-dim hypergrid.
  • A necessary condition is for it to be a simplex in the triangulation of the original hypergrid.
Issue 2  The triangulation of the d-dimensional hypergrid (embedded in the snake $W$) should be consistent with its corresponding triangulation of the (d+1)-dimensional hypergrid.

Going back to Algorithm 2, any edge between a color $(d+1)$ node with any node of other colors is introduced by $\mathbf{L}^2(T, u)$ between a node of $p_{d+1} = 0$ and another of $p + d + 1 = 1$. The latter is on a base hypercube separated on the original hypercube. This relationship is maintained in the next step of Algorithm 3. Through the map $\psi$ in Algorithm 3 an $(d+1)$-simplex of panchromatic colors of the $(d+1)$ dimensional space $W$ relates to the original $d$-dimensional hypergrid. As no mapped node of color $(d+1)$ is in the image of the original $d$-dimensional hypergrid, we obtain the resulting $d$-dim simplex in the original space by the image of $\psi$ on the remained $d$ vertices in the $(d+1)$ space. This concludes the discussion on the above Issue 1.

To handle Issue 2, we make use of the Kuhn triangulation [28].

**Definition 19** *(Kuhn triangulation).* Consider Unit Hypercube $H^k = (\{0,1\}^k, E^k)$, where $\forall \vec{a}, \vec{b} \in H^k, (\vec{a}, \vec{b}) \in E^k$ iff $\exists i : |\vec{a} - \vec{b}| = \vec{e}_i$. Let $S_k$. be the set of all permutations on $\{1, 2, \cdots, k\}$.

• $\forall \alpha \in S_k$, $\alpha = \begin{pmatrix} 1 & 2 & \cdots & k \\ \alpha_1 & \alpha_2 & \cdots & \alpha_k \end{pmatrix}$, we define base simplex $S(\alpha)$ on $k+1$ pints, in $[0,1]^k$, $\Delta(\alpha) = convex\text{-}hull(\vec{0}, \vec{0} + \vec{e}_{\alpha_1}, \vec{0} + \vec{e}_{\alpha_1} + \vec{e}_{\alpha_2}, \cdots, \vec{0} + \vec{e}_{\alpha_1} + \vec{e}_{\alpha_2} + \cdots + \vec{e}_{\alpha_k})$

$KT([0,1]^k) = \cup_{\forall \alpha \in S_k} \Delta(\alpha)$ is a partition of $[0,1]^k$ and called the Kuhn partition of the unit hypercube $[0,1]^k$.

Consider the construction the Kuhn triangulation on each unit hypercube in the dicephalic snake structure in Fig. 8.

We base on the origin $(x_1, x_2, \cdots, x_{d+1}) = (0, 0, \cdots, 0)$ to create our Kuhn triangulations. On each unit base hypercube, we move from the node with the minimum total sum of the absolute values of its coordinate to the node with the maximum total sum of absolution values of its coordinates. This way, we have the same triangulations on the intersection of every two adjacent unit hypercubes in the dicephalic snake structure in Fig. 8. Therefore, they connect consistently this way. The required property holds except for the reversing face, which we consider next.

Finally, we consider $t = 1$ and $t = 2$, respectively. At each layer, the steps to identify $(r_1, x_2, \cdots, x_{d+1})$ with $(-r_1, -x_2, \cdots, x_{d+1})$ will not change the maximum nor the minimum of the absolute values at $(r_1, r_2)$ and $(-r_1, -r_2)$ at each layer $x_{d+1}$. The triangulations on the surfaces will remain the same.

## 6. Oracle computational complexity

We have established that the computational complexity of finding a discrete fixed point, such as a Sperner's base simplex, is PPA-complete. Here the color of a vertex is computed using an input Boolean circuit of polynomial size.

Alternatively, in the oracle model, the color is given by an oracle in one time unit. Below we prove that the number of queries made to the oracle in order to find a Sperner base triangle on the Möbius band of size $N \times N$ is $\Theta(N)$. The same result can be extended to the general $d$-dimensional non-orientable space, i.e., finding a $d$-dimensional Sperner simplex in a non-orientable space of size $N^d$ requires $\theta(N^{d-1})$ queries to be made to the oracle. We refer the query time to the oracle time complexity.

Such a matching bound was known for the orientable space of all constant dimension spaces (see Table 2). The idea was based on the oddity of the index of the colored input grid. The extension to the non-orientable space is based on their close tie. Here we discuss the oracle computational complexity for finding a Sperner base simplex on the Möbius band.

**Theorem 8.** *For a triangulated $N \times N$ Möbius band with an odd boundary index with its colors given by an oracle function, there is an algorithm that finds a Sperner simplex in time $O(N)$. On the other hand, there is an instance for which any algorithm would take time $\Omega(N)$.*

**Proof.** For the upper bound, we adopt the divide-and-conquer by partitioning the grid into four pieces of $\frac{N}{2} \times \frac{N}{2}$ each. At least one of the four pieces has an odd number of edges of colors $\{1, 2\}$, as the original grid is odd. To find that one piece, we only need to count the number of {1,2} edges for three of the pieces at most. Therefore, a total query time of $5N$ can reduce the original problem to one of size $N/2$. We have $T(N) = 5N + T(N/2)$. In time $10N$, we end up with a unit square of index 1 which is divided into two base triangles. One of them must have index 1 while the other must have index 0. Therefore, the index 1 base triangle is a fully colored Sperner base triangle.

For the lower bound, for any algorithm $A$ that returns a Sperner base triangle on a triangulated Möbius band of index 1, we use that algorithm to solve the same problem of finding a Sperner base triangle on an orientable grid. Here is the idea: we take two edges centrally symmetric to each other on the boundary of the $N \times N$ grid. Extend them properly into a long ladder to meet in the middle to merge after twisting the edge 180 degree. The resulting object is roughly a Möbius band. For each edge of two, we can make its two end nodes of the same color from $\{1, 2\}$. The index of the closed boundary will change by 0 or 2. Its oddity will not change. Finding a base pan-chromatic triangle on the new surface will also be a base pan-chromatic triangle in the original orientable grid. As finding a Sperner base triangle on an orientable grid is known to take $\Omega(N)$ time in the worst case [15], the lower bound result follows. □

The same analysis can be generalized to derive the following results.

**Corollary 1.** *Finding a d-dimensional discrete fixed point (including Sperner Brouwer, DPZP, simple Tucker, etc.) in a non-orientable space of size $N^d$ requires $\theta(N^{d-1})$ queries to be made to the oracle.*

## 7. Remarks and discussion

We have discussed two types of discrete fixed point problems on the Möbius band: finding one, and given one finding another, depending on the boundary conditions. We show that both problems are PPA-complete for several versions of discrete fixed point problems, including the DPZP, Sperner, Brouwer and the simple Tucker problem on the 2D Möbius band.

Our first step focused on the 2D version. We started with DPZP, that requires finding a zero point in a discrete version of the continuous functions. Based on this result, we derived PPA-completeness proofs for several other related fixed point problems on the Möbius band. We discussed given one finding another type of discrete fixed point problems for Möbius Sperner and Brouwer. We discussed finding one for the simple Tucker and DPZP. Actually, these two types of discrete fixed point problems are exchangeable. For example, we can change all negative colored vertices to color 0 in DPZP to obtain a "finding one" version for Möbius Sperner. We left those cases out and only described useful structures and techniques for the typical cases.

In this work, the link between a non-orientable topological space and an undirected path following computational paradigm introduced by Grigni [11], is further validated with the simple structure of the 2D Möbius band. The work deepens our understanding of the differences in computational complexity between the two classes PPAD and PPA in terms of the underlying topological structures.

The simplicity of our construction means that it can be extended beyond the 2D Möbius band to more general cases. For example, the PPA completeness of given one finding another fixed point version extends naturally to the Klein bottle [27], the projective space, and other non-orientable surfaces. Simplicity has played a key role in raising further curiosities from the 2D Sperner work of Chen and Deng [15] in the orientable space, such as in Mehta [29] and Goldberg [30].

Further, the results can be extended to higher dimensions, even for the case where each side is of a constant length. One such case of given one finding another fixed point in a higher dimensional non-orientable space has been presented in Section 5. The result extends to different related solution concepts. The technique has further developed in a subsequent paper to derive the PPA-completeness proof for finding a complete edge in the octahedral Tucker problem by Deng et al. [31], a high dimension version of the Tucker problem with size length two, its smallest possible non-trivial version for any dimension.

The discrete fixed point problems in our discussion have an exponential size configuration. Otherwise, we can enumerate the space to find a solution by brute-force search. To compute colors and function values, a polynomial size circuit is given as input. Alternatively, an oracle model returns those values in one unit oracle time (see Hirsch et al. [17]). Chen and Deng [13] proved that there is an asymptotic matching bound for finding Brouwer's fixed point in Euclidean space. The matching bound was extended to other discrete fixed point problems by Deng et al. [14]. The same matching bound applies for the non-orientable spaces we discussed here. The lower bound holds simply because the problem is more difficult to solve in the non-orientable spaces. The upper bound follows by applying the standard divide-and-conquer method to the index adopted for the non-orientable spaces.

Hopefully, the natural 2D Möbius Sperner will encourage future research to develop a better knowledge of the PPA class. In particular, as had suggested by Grigni [11], we would also like to see the computational complexity of the Smith's Theorem, which is known in the class of PPA, be eventually completely characterized.

The Smith's Theorem states that given a Hamiltonian cycle $H = (v_1, v_2, \cdots, v_n)$ in a graph $G = (V, E)$ of all degree three vertices, there is another Hamiltonian cycle. A PPA-structure can be constructed accordingly as follows. We define a Hamiltonian path $P = (a_1, a_2, \cdots, a_n)$ rooted at a node $a_1$ (fixed) and its associated edge $(a_1, a_2)$ as a super node of the PPA structure. As $a_n$ is of degree 3, it is connected to two other vertices, $a_i, a_j$. Then in the PPA structure, it is connected to two super-nodes. One is the Hamiltonian path $(a_1, a_2, \cdots, a_i, a_n, a_{n-1}, \cdots, a_{i+1})$ and another is the Hamiltonian path $(a_1, a_2, \cdots, a_j, a_n, a_{n-1}, \cdots, a_{j+1})$. If one of $\{a_i, a_j\}$ is $a_1$, one of the two Hamiltonian paths is a cycle, and $P$ is a super-node of degree 1 in the PPA structure.

As the super-node of the PPA structure is a Hamiltonian path with a specified root $a_1$ with a fixed edge $(a_1, a_2)$, each super-node has at most two neighboring super-nodes. The super-nodes with the same fixed starting node in the Hamiltonian path and their neighboring Hamiltonian paths form a PPA-structure. It is clear that the number of super-nodes as end of lines in this PPA-structure is even, once the root node for the Hamiltonian paths is fixed.

As each end of line super-node in the PPA structure corresponds to a Hamiltonian path with a specified "starting" node is even, the number of cycles with a node specified is even. However, it is obvious that $K_4$ contains exactly 3 different Hamiltonian cycles, we cannot generally claim a Smith graph has an even number of Hamiltonian cycles.

Recently, new and interesting PPA-complete problems are discovered in [21], [32], [31], [33] and [34]. It is still desirable to answer the challenge to prove SMITH to be PPA-complete.

## Declaration of competing interest

## Acknowledgments

## References

[1] C. Lemke, J.T. Howson, Equilibrium points of bimatrix games, J. Korea Soc. Ind. Appl. Math. 12 (2) (1964) 413–423.
[2] R.W. Cottle, G.B. Dantzig, Complementary pivot theory of mathematical programming, Linear Algebra Appl. 1 (1) (1968) 103–125.
[3] C.H. Papadimitriou, On the complexity of the parity argument and other inefficient proofs of existence, J. Comput. Syst. Sci. 48 (3) (1994) 498–532.
[4] X. Chen, X. Deng, S.-H. Teng, Settling the complexity of computing two-player Nash equilibria, J. ACM 56 (3) (2009) 14:1–14:57.
[5] S. Kintali, A compendium of PPAD-complete problems, http://www.cs.princeton.edu/~kintali/ppad.html, 2016. (Accessed 3 March 2016) [Online].
[6] A. Thomason, Hamiltonian cycles and uniquely edge colourable graphs, in: B. Bollobás (Ed.), Advances in Graph Theory, in: Annals of Discrete Mathematics, vol. 3, Elsevier, 1978, pp. 259–268.
[7] K. Cameron, J. Edmonds, Some graphic uses of an even number of odd nodes, Ann. Inst. Fourier 49 (3) (1999) 815–827.
[8] C. Chevalley, Démonstration d'une hypothèse de M. Artin, Abh. Math. Semin. Univ. Hamb. 11 (1) (1935) 73–75.
[9] N. Alon, Combinatorial nullstellensatz, Comb. Probab. Comput. 8 (1–2) (1999) 7–29.
[10] E. Jeřábek, Integer factoring and modular square roots, CoRR, arXiv:1207.5220 [abs], 2012.
[11] M. Grigni, A Sperner lemma complete for PPA, Inf. Process. Lett. 77 (5–6) (2001) 255–259.

[12] K. Friedl, G. Ivanyos, M. Santha, Y.F. Verhoeven, Locally 2-dimensional Sperner problems complete for the polynomial parity argument classes, in: Algorithms and Complexity, in: Lecture Notes in Comput. Sci., vol. 3998, Springer, Berlin, 2006, pp. 380–391.
[13] X. Chen, X. Deng, Matching algorithmic bounds for finding a Brouwer fixed point, J. ACM 55 (3) (2008) 26, Art. 13.
[14] X. Deng, Q. Qi, A. Saberi, J. Zhang, Discrete fixed points: models, complexities, and applications, Math. Oper. Res. 36 (4) (2011) 636–652.
[15] X. Chen, X. Deng, On the complexity of 2D discrete fixed point problem, Theor. Comput. Sci. 410 (44) (2009) 4448–4456.
[16] R. Savani, B. von Stengel, Hard-to-solve bimatrix games, Econometrica 74 (2) (2006) 397–429.
[17] M.D. Hirsch, C.H. Papadimitriou, S.A. Vavasis, Exponential lower bounds for finding Brouwer fix points, J. Complex. 5 (4) (1989) 379–416.
[18] A. Krawczyk, The complexity of finding a second Hamiltonian cycle in cubic graphs, J. Comput. Syst. Sci. 58 (3) (1999) 641–647.
[19] K. Cameron, Thomason's algorithm for finding a second Hamiltonian circuit through a given edge in a cubic graph is exponential on Krawczyk's graphs, Discrete Math. 235 (1–3) (2001) 69–77, Chech and Slovak 3.
[20] J. Edmonds, L. Sanità, On finding another room-partitioning of the vertices, Electron. Notes Discrete Math. 36 (2010) 1257–1264.
[21] J. Aisenberg, M.L. Bonet, S. Buss, 2-d tucker is PPA complete, Electron. Colloq. Comput. Complex. 22 (2015) 163.
[22] Goldman Crescenzi, Piccolboni Papadimitriou, Yannakakis, On the complexity of protein folding (extended abstract), in: STOC: ACM Symposium on Theory of Computing, STOC, 1998.
[23] S. Even, A.L. Selman, Y. Yacobi, The complexity of promise problems with applications to public-key cryptography, Inf. Control 61 (2) (1984) 159–173.
[24] O. Goldreich, On promise problems, Electron. Colloq. Comput. Complex. 18 (2005).
[25] H.E. Scarf, The approximation of fixed points of a continuous mapping, Cowles Foundation Discussion Paper 216R, Cowles Foundation for Research in Economics, Yale University, 1967.
[26] M.J. Todd, The Computation of Fixed Points and Applications, vol. 124, Springer-Verlag, Berlin, Heidelberg, 1976.
[27] E.W. Weisstein, Klein bottle, http://mathworld.wolfram.com/KleinBottle.html, 2016. (Accessed 3 March 2016) [Online].
[28] K. Kuhn, Some combinatorial lemmas in topology, IBM J. Res. Dev. 4 (5) (1960) 518–524.
[29] R. Mehta, Constant rank bimatrix games are ppad-hard, in: Proceedings of the 46th Annual ACM Symposium on Theory of Computing, STOC '14, ACM, New York, NY, USA, 2014, pp. 545–554.
[30] P.W. Goldberg, The complexity of the path-following solutions of two-dimensional Sperner/Brouwer functions, CoRR, arXiv:1506.04882 [abs], 2015.
[31] X. Deng, Z. Feng, R. Kulkarni, Octahedral Tucker is PPA-complete, Electron. Coll. Comput. Compl. TR17-118 (2017).
[32] A. Belovs, G. Ivanyos, Y. Qiao, M. Santha, S. Yang, On the polynomial parity argument complexity of the combinatorial Nullstellensatz, in: CCC 2017, 2017.
[33] A. Filos-Ratsikas, P.W. Goldberg, Consensus halving is PPA-complete, in: Proceedings of the 50th Annual ACM SIGACT Symposium on Theory of Computing, 2018, pp. 51–64.
[34] A. Filos-Ratsikas, S.K.S. Frederiksen, P.W. Goldberg, J. Zhang, Hardness results for consensus-halving, in: 43rd International Symposium on Mathematical Foundations of Computer Science, MFCS 2018, Schloss Dagstuhl-Leibniz-Zentrum fuer Informatik, 2018.